T-AM-Min1 INTRACELLULAR SIGNALLING. Larry A. Sklar, Dept. of Immunol. Scripps Clinic and Research Foundation, La Jolla, CA 92037

The interaction of receptors with stimuli (photons, hormones, growth factors, etc.) initiates the biochemistry of cell activation. Activated receptors in many cell types are coupled to guanyl nucleotide binding proteins which control either adenylate cyclase or a phosphodiesterase (Stryer). The substrate for the phosphodiesterase is cGMP in the visual photoreceptor (Stryer). However, a more general action of the coupling proteins could be to stimulate phospholipase C (itself a phosphodiesterase) and thus, turnover phosphatidylinositol, produce the messengers diacylglycerol and inositoltrisphosphate, and ultimately, release intracellular stores of Ca^{++} (Williamson). The action of intracellular signals has been studied in permeabilized cells, isolated organelles (Williamson), by microinjection and by photoactivatable signal precursors (Lester). The targets of the signals are often kinases which phosphorylate and modulate the activities of intracellular phosphoproteins as well as the receptors themselves (Staros). Precise control of photoreceptor activation has been accomplished with precise control over the light source. It is now possible to control the rate and number of receptors activated by "real" ligands (Sklar). In addition, novel spectroscopic procedures have been developed which permit the real-time, continuous analysis of ligand-receptor dynamics (association, dissociation, internalization) on cells with typical numbers of receptors (i.e. 50,000) (Sklar).

In this minisymposium, the speakers will explore the details of the signalling pathways and ligand-receptor dynamics. We will show how the control of both signalling events and binding interactions may be used to probe cell activation and to develop concepts by which activation is regulated. We will address the questions "How many, how fast, how long, what, and where?"

T-AM-Min2 SIGNAL-COUPLING PROTEINS IN AMPLIFICATION CASCADES. Lubert Stryer, Department of Cell Biology, Stanford University School of Medicine, Stanford, California 94305.

The photoexcitation of rhodopsin triggers a cascade that results in the rapid hydrolysis of a large number of molecules of cyclic GMP. Transducin, a multisubunit peripheral membrane protein, is the information-carrying intermediate in the activation of the cyclic GMP phosphodiesterase. Photoexcited rhodopsin (R^*) catalyzes the exchange of GTP for GDP bound to the α-subunit of transducin (T). About 500 molecules of T_α-GTP are formed per absorbed photon at low light levels. T_α-GTP, released from the β and γ subunits of transducin, then activates the phosphodiesterase by relieving an inhibitory constraint imposed by its small subunit. Each activated phosphodiesterase molecule hydrolyzes more than a thousand cyclic GMP per second, giving an overall gain of more than 500,000. Photoexcited rhodopsin triggers the activation of a molecule of transducin in a millisecond, which is sufficiently rapid to enable this cascade to participate in visual excitation. Hydrolysis of GTP bound to T_α serves to restore the system to the dark state. Transducin, like the G proteins of the adenylate cyclase cascade, can be specifically ADP-ribosylated by cholera toxin and pertussis toxins. In both cascades, labeling by pertussis toxin blocks the capacity of transducin to interact with the excited receptor, whereas labeling by cholera toxin inhibits the hydrolysis of bound GTP, leading to persistent activation. Moreover, the molecular design of the hormone-triggered cyclic AMP cascade is similar to that of the light-triggered cyclic GMP cascade. It seems likely that transducin, the stimulatory G protein, the inhibitory G protein, and the ras protein are members of the same family of signal-amplifying proteins.

T-AM-Min3 INOSITOL TRISPHOSPHATE AND DIACYLGLYCEROL AS INTRACELLULAR SECOND MESSENGERS IN LIVER. John R. Williamson, Suresh K. Joseph, Andrew P. Thomas and Ronald H. Cooper. Univ. of Pennsylvania, Dept. of Biochemistry and Biophysics, Philadelphia, Pennsylvania 19104 USA.

Recent studies have established that receptor occupation by a variety of Ca^{2+}-mobilizing hormones such as α_1-adrenergic agents, vasopressin, and angiotensin II causes a rapid phosphodiesterase mediated hydrolysis of phosphatidylinositol-4,5-bisphosphate (PIP_2) with the production of the water soluble compound myo-inositol-1,4,5-trisphosphate (IP_3) and the lipophilic molecule 1,2-diacylglycerol (DG). It has now become apparent that each of these compounds have separate and distinct roles as intracellular second messengers. IP_3 causes the mobilization of intracellular Ca^{2+} from a specialized sub-population of the endoplasmic reticulum, and is thus responsible for the rapid rise of the cytosolic free Ca^{2+} and subsequent activation of phosphorylase. The hormone-induced increase of DG activates protein kinase C, which is also directly activated by phorbol esters such as PMA. Addition of PMA to hepatocytes caused increased phosphorylation of two 16,000 dalton proteins with pI values of 5.80 and 6.40 and three proteins of Mr values 68,000, 52,000, and 36,000. Vasopressin increased the phosphorylation of these three proteins plus the 16,000 dalton protein with a pI of 5.80, while phenylephrine increased the phosphorylation of only the 16,000 dalton protein with a pI of 6.40. Addition of PMA to hepatocytes had no effect on the cytosolic free Ca^{2+} or Ca^{2+} fluxes across the plasma membrane, but greatly inhibited the α_1-adrenergic-mediated increase of cytosolic free Ca^{2+} with little effect on the vasopressin response. These results suggest that a phosphorylated substrate of protein kinase C is involved either in regulation of hormone binding to the α_1-receptor or in the receptor-mediated activation of the plasma membrane phosphodiesterase.

T-AM-Min4 USE OF FLASH-ACTIVATED INTRACELLULAR MESSENGERS TO STUDY THE GATING OF ION CHANNELS. H. A. Lester, Division of Biology 156-29, Caltech, Pasadena, CA 91125

Because putative intracellular messengers cannot be applied quickly and reversibly to the interior of intact cells, there is little information about spatial localization and kinetics of action of these molecules. Several reseach groups are now approaching this problem by employing molecules that are themselves inert but release the messenger of interest upon illumination. If the precursor molecules are uncharged, they can cross the membrane by diffusion from the external solution; if charged, they can be introduced by microinjection or by diffusion from a patch pipette. The most common strategy is to "cage" the messenger with the photosensitive o-nitrobenzyl group. The photolyses go to completion on a time scale of 10^{-3} s to 1 s. The 4,5-dimethoxy-2-nitrobenzyl and the 2,6-dinitrobenzyl moieties are especially useful from the viewpoint of action spectrum and photolytic speed. The approach has been successful with phosphodi- and triesters that produce nucleotides upon photolysis. For instance, when cAMP is photoreleased inside heart cells, there are detectable increases in Ca currents within 100 ms; 10-20 s are required for the full effects. Tsien has synthesized an o-nitrobenzyl derivative of BAPTA that changes its K_D for Ca from 0.17 μM to 7 μM upon irradiation; when photolyzed inside cells, this molecule liberates Ca which then activates K channels (Tsien & Zucker). Other uses of light-activated intracellular messengers will be discussed. Supported by AHA and by GM-29836.

T-AM-Min5 RECEPTOR/KINASES IN TRANSMEMBRANE SIGNALING. James V. Staros, Vanderbilt University, Department of Biochemistry, School of Medicine, Nashville, TN 37232

Epidermal growth factor (EGF) is a 53 residue mitogenic polypeptide. On binding to its plasma membrane receptor, it elicits a wide range of cellular responses. Some of these responses, e.g., modulation of membrane transport systems, occur rapidly, while others, e.g., stimulation of macromolecular synthesis and, ultimately, mitosis, occur after a lag time of hours. One of the most rapid measurable responses to the binding of EGF is the stimulation of a protein kinase which is specific for tyrosyl residues. Studies in our laboratory have shown that this EGF-stimulable protein kinase is part of the same polypeptide as is the EGF receptor. We have hypothesized that the EGF receptor/kinase is disposed as a transmembrane allosteric enzyme with the effector site -the EGF binding site - accessible to the extracellular milieu and the active site accessible to the cytoplasm. We have proposed that the allosteric activation of the kinase by EGF is a primary transmembrane signaling event. The recent discoveries by other workers of receptor-associated kinases for insulin and for platelet-derived growth factor suggest that this model for transmembrane signaling may have some generality. Several groups have cloned and sequenced cDNAs to the mRNA for the EGF receptor/kinase, resulting in a derived primary sequence for the receptor/kinase. These sequence data can now be incorporated into models for the structure of this molecule which may help to elucidate the mechanism of transmembrane signaling. Supported by the NIH, AM25489.

T-AM-Min6 SIGNAL TRANSDUCTION AND LIGAND RECEPTOR DYNAMICS IN THE HUMAN NEUTROPHIL. Larry A. Sklar, Dept. of Immunology, Scripps Clinic and Research Fdn., La Jolla, CA 92037

We have developed real-time methods to analyze and control ligand-receptor interaction on cells in suspension. We use fluorescence flow cytometry and spectrofluorometry to study the binding of a fluoresceinated N-formyl chemotactic hexapeptide. The interaction between ligand and receptor is described as:

$$L + R \underset{5/\text{min}}{\overset{10^9/\text{M min}}{\rightleftharpoons}} LR^* \xrightarrow[0.3/\text{min}]{2.5/\text{min}} LR_o \xrightarrow{0.2/\text{min}} LR_{int}$$

The active ligand-receptor complex (LR*) has a life-time of ~5 seconds, and then decays into an inactive state (LR_o) immobilized on the cell cytoskeleton prior to its internalization (LR_{int})

We control ligand-receptor interaction using "ramp" and "pulse" protocols of stimulation. The "pulse" takes advantage of a high affinity antibody to fluorescein which complexes the free fluorescent peptide and interrupts ligand binding at the receptors. Neutrophil signals (e.g. Ca^{++}) and responses (e.g. free radical production) are transient in a pulse and decay to baseline following a latency period comparable to the lifetime of the activated receptor. These transient events have intriguing implications for the regulation of cell function. For example, when ligand is administered in a ramp so that a few percent of the receptors are occupied per minute, the magnitude of the signal and the response depend upon the rate. This loss of magnitude occurs because the magnitude of the signals (and coupled responses) are governed by the rate of generation (a function of the binding rate) and the rate of decay. Since signal (Ca^{++}) can restore function to Ca^{++}-depleted cells only during the time when LR* is present, we believe that a second transient signal arising from LR* (perhaps diacylglycerol) must also be present.

Signaling Luncheon: Roger Tsien — Featured Speaker. See Abstract Page 193a.

T-AM-A1 ELECTRONIC COUPLING BETWEEN THE MANGANESE MULTILINE EPR CENTER AND A PARAMAGNETIC NEIGHBOR IN O_2 EVOLVING PHOTOSYNTHETIC MEMBRANES. G. C. Dismukes and R. Damoder, Princeton University, Dept. of Chemistry, Princeton, NJ 08544

A multiline EPR signal arising from a manganese cluster having 2 or 4 Mn ions occurs in O_2-evolving photosynthetic membranes. Formation of the EPR signal by 200 K illumination in dark-adapted samples creates a spectrum having 18-19 peaks. The temperature dependence, microwave saturation and number of peaks change as a function of the illumination history. Fewer peaks and reduced intensity are observed for shorter dark-adaptation periods indicating changes in the environment about manganese. These properties differ from those observed for synthetic Mn dimers such as $[Mn(III,IV)O]_2L_4$ (L=bipy,phen) which are currently the simplest models. The synthetic dimers exhibit only 16 peaks. Their EPR signals saturate at lower microwave power [p_{max}=5 mW(10K)] compared to the multiline signal [p_{max}=36mW(10K). The temperature dependence of their EPR signals exhibits normal Curie behavior for kT<<J=100-150 cm^{-1} where J is the Heisenberg exchange energy between the two Mn ions (Fig.) The intensity of the multiline signal peaks at 6±1K and disappears at lower temperature, indicating a non-paramagnetic ground state (Fig.) Simulation of this temperature dependence is shown for a model in which a manganese dimer (site a) interacts with another paramagnet (site b) to produce a non-EPR active state for kT<J_{ab} (J=17 cm^{-1}, J_{ab}=3-4 cm^{-1}, Fig.) The site b paramagnet is unidentified but may be another manganese site, Cu^{2+}, or Fe^{3+}. Supported by NSF CHE 82-17920 and a Searle Scholars Award.

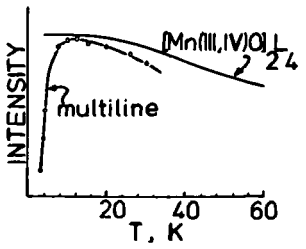

T-AM-A2 A NEW ELECTRONIC TRANSITION DUE TO MANGANESE IN O_2 EVOLVING MEMBRANES. G. C. Dismukes and Paul Mathis, Serv. de Biophysiques CEN-Saclay, France and Dept. of Chemistry, Princeton University, Princeton, NJ 08544

A new electronic transition has been detected in the near infrared (IR) spectrum in O_2 evolving photosynthetic membranes from spinach. This transition oscillates in yield with a period of four when generated by a train of short flashes exposed to a dark-adapted (synchronized) population of membranes (S_1 state). This is seen in Fig. 1. This is analogous to the period four oscillation of O_2 yield and the manganese multiline EPR signal for the presumed catalytic site in the state S_2 (after 1 flash). Removal of manganese by NH_2OH abolishes the IR signal, the EPR signal and O_2 evolution. Removal of proteins of 17- and 24 kDa by salt washing removes the IR signal, but this is partially reversed by 10 mM $CaCl_2$. The yield of the state exhibiting the IR absorption correlates most closely with the sum of S_2+S_3. Comparison of the spectrum of the oscillating component (Y_5-Y_4) to that of two different synthetic manganese dimers poised in the mixed-valent state Mn_2(III, IV), reveals close correspondence with the intervalence electronic transition $Mn_2(III,IV) \xrightarrow{h\nu} Mn_2(IV,III)$. Supported by CEN-Saclay and NSF-CHE 82-17920.

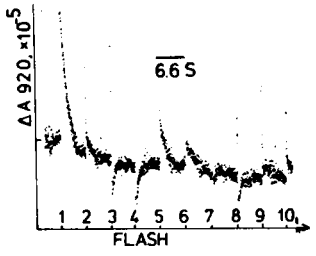

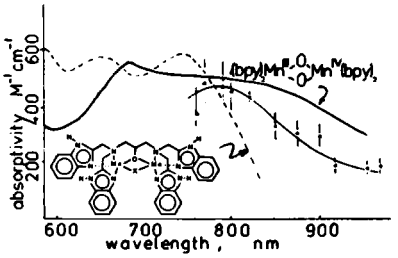

T-AM-A3 CORRELATION BETWEEN A 33 kDa MANGANOPROTEIN, THE S_2 MULTILINE EPR SIGNAL AND PHOTOSYNTHETIC O_2 EVOLUTION. D. A. Abramowicz, R. Damoder and G. Charles Dismukes, Dept. of Chemistry, Princeton University, Princeton, NJ 08544

O_2 is released from green plants during photosynthesis with a yield which cycles with a period of four when produced by a train of short flashes (peaks:3,6,11...). A multiline EPR signal due to a binuclear manganese site also oscillates in yield with a period of four (peaks: 1,5...) and has been attributed to the catalytic site for water oxidation (G.C. Dismukes and Y. Siderer. 1981. PNAS 78, 274). This signal disappears concomitant with loss of O_2 evolution induced by the removal of 2 Mn by NH_2OH or by removing a 33 kDa extrinsic protein either by alkaline salt washing or by osmotic shock (Fig.). Extraction of this protein releases 2 Mn atoms. Prior removal of two proteins of 17 and 24 kDa does not reduce the multiline EPR signal. When isolated in the presence of chemical oxidants the 33 kDa protein binds 1.7 ± 0.3 Mn. It is capable of reconstituting 25% of lost oxygen evolution activity to osmotically shocked membranes and 55% reconstitution (310 µmoles O_2·mg Chl^{-1}·h^{-1}) to PS-II membranes depleted of all three proteins by alkaline salt washing. This reconstitution is blocked by NH_2OH which reduces manganese to the labile Mn(II) oxidation state. Supported by NSF CHE 82-17920 and a Searle Scholars Award.

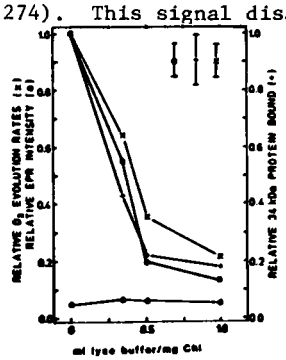

T-AM-A4 A SURFACE-ENHANCED RAMAN SIGNAL ASSOCIATED WITH MANGANESE IN PS II MEMBRANES. M. Seibert, T. M. Cotton,* and J. G. Metz, Solar Energy Research Institute, Golden, CO 80401, and *University of Nebraska, Lincoln, NE 68588.

Manganese is required for photosynthetic O_2 evolution and is associated with the active site of the oxygen-evolving complex in Photosystem II (PS II). We report here a new surface-enhanced Raman signal detected in spinach oxygen-evolving PS II membranes treated with 1 M $CaCl_2$. This treatment removes three extrinsic proteins from the membrane but does not extract functional Mn (1). The signal is not seen in Tris-treated preparations, which retain none of the three proteins nor Mn. In addition, it is also not seen in NaCl-treated preparations, which retain Mn and the 33-kDa extrinsic protein. The Raman signal is unstable and is related kinetically to the release of about half the Mn found initially in the $CaCl_2$-treated material. It is not yet possible to determine whether the Raman signal is a direct or indirect monitor of the pool of unstable Mn. However, the source of the signal is located between the 33-kDa extrinsic protein and the PS II membrane, probably at the site of the 34-kDa intrinsic protein (2). Results with membranes isolated from Scenedesmus WT and non-O_2-evolving mutant cells will also be presented.

(1) Ono, T.-A., and Y. Inoue. 1983. FEBS Lett. 164:255.
(2) Metz, J. G., and M. Seibert. 1984. Plant Physiol. In Press.

Supported by the Biological Energy Research and Chemical Sciences Divisions of OER/DOE.

T-AM-A5 MAGNETIC PROPERTIES OF MANGANESE IN THE PHOTOSYNTHETIC OXYGEN-EVOLVING CENTER. Julio C. de Paula and Gary W. Brudvig, Dept. of Chemistry, Yale University, New Haven, Connecticut 06520.

The magnetic environment of the manganese active site of the oxygen-evolving complex (OEC) of Photosystem II (PSII) is investigated by means of the continuous power saturation and temperature dependence of three EPR signals which are associated with the S_2 state of the OEC. It is found that illumination at 200 K for 2 min of PSII membranes which are incubated in the dark for 4 hrs at 0^oC generates an S_2 state EPR signal which saturates easily and exhibits a non-Curie temperature dependence at non-saturating conditions. On the other hand, 6 min dark adapted samples illuminated at 160 K produce a signal which saturates at higher microwave powers and exhibits no intensity maximum in the 4.0-16.0 K temperature range under non-saturating conditions. Furthermore, illumination at 170 K of short-term dark adapted PSII membranes generates a signal which is not saturated with our current experimental setup and exhibits non-Curie behavior. We conclude that each EPR spectrum originates from a thermally excited state of one of three distinct configurations of the manganese active site. The temperature dependence data is fitted to a model in which two paramagnetic sites are ferromagnetically coupled. All three sets of data can be accounted for by varying the magnitude of the superexchange coupling constant. (Supported by the Searle Scholars Fund, USDA-CRGO, Dreyfus Foundation, Research Corporation, PRF.)

T-AM-A6 EFFECT OF ANAEROBIC CONDITIONS ON THE MANGANESE SITE OF THE OXYGEN-EVOLVING COMPLEX OF PHOTOSYSTEM II. Warren F. Beck and Gary W. Brudvig (Intr. by Peter B. Moore), Department of Chemistry, Yale University, New Haven, Connecticut 06511.

Removal of dioxygen causes reversible changes in the Mn site in the oxygen-evolving complex (OEC) of photosystem II (PSII) observable using low-temperature EPR spectroscopy of the S_2 state. The presence or absence of dioxygen affects the power saturation and temperature dependence of the S_2 state EPR signals produced by 160-200K illumination of spinach PSII membranes only if dioxygen is replaced by a nitrogen atmosphere shortly following illumination; extensively dark-adapted (4 hrs dark incubation at 0 C) membranes exhibit S_2 state EPR signals following illumination independent of the presence or absence of dioxygen. These results are consistent with the observation that the Mn site of the OEC undergoes a change from an active state capable of oxygen consumption following illumination to a resting state incapable of oxygen consumption, affecting the nature and illumination dependence of the S_2 state EPR signals produced following illumination (W. Beck, J. de Paula, and G. Brudvig, submitted). The change in the Mn site upon removal of dioxygen in the active state is also consistent with the observation that anaerobic conditions reversibly affect the rate of ferricyanide reduction in chloroplasts (Popovic et al., Photochem. Photobiol. (1984), 377-380). These results suggest that the OEC is affected by removal of dioxygen through a mechanism that alters the environment of the Mn site. (Supported by the Searle Scholars Fund, USDA-CRGO, Dreyfus Foundation, Research Corporation, PRF).

T-AM-A7 INHIBITORS AFFECTING THE OXIDIZING SIDES OF PHOTOSTEM II AT THE Ca^{2+} AND Cl^- SENSITIVE SITES.

H.Y. NAKATANI+ AND R. CARPENTIER. MSU-DOE Plant Research Laboratory, Michigan State University, East Lansing, MI 48824, +Present Address: Philip Morris, USA, Research Center, P.O. Box 26583, Richmond, Va. 23261

In addition to compounds which inhibit the function of calmodulin (a ubiquitous calcium regulatory protein found in plants and mammalian tissues), Ca^{2+} and Cl^- channel blockers of mammalian tissues were also found to inhibit electron transport in Triton X-100 extracted photosystem II submembrane preparations from spinach. Their inhibitory action was overcome by electron donation to P680 by diphenylcarbazide or H_2O_2. The inhibitory effect of trifluoperazine, however, could not be overcome by this latter donor. The presence of Ca^{2+} and/or Cl^- also partially prevented their inhibitory action. We postulate that the inhibitory action of these compounds occurs at the level of the oxygen evolving complex (OEC) at the site of Ca^{2+} -regulation of the Cl^- -cofactor requirement in oxygen evolution (see H.Y. Nakatani, Biochem. Biophys. Res. Comm., 1984, 120, 299-304).

T-AM-B1 FUSION ASSAYS: LIPID EXCHANGE, AGGREGATION, LIPID MIXING, OR COALESCENCE OF CONTENTS? T. M. Allen and N. Düzgüneş, Cancer Research Institute, University of California, San Francisco, CA 94143 (ND) and Pharmacology Dept., University of Alberta, Edmonton T6G 2H7 (TA).

A fusion assay which monitors the mixing of aqueous contents (CM) of two separate liposome populations encapsulating Tb or dipicolinic acid, and a fusion assay for the mixing of lipids (LM) measuring resonance energy transfer (RET) between NBD-Phosphatidylethanolamine (PE) and Rhodamine-PE, were compared with respect to kinetics. LM was followed by methods resulting either in dequenching of NBD fluorescence (LMD) or fluorescence quenching (LMQ). The initial rates of CM and LM, induced by Ca^{2++}, Mg^{2+} and Sr^{2+} in large unilamellar vesicles (LUV, 100 nm diameter) composed of phosphatidylserine (PS), PS:phosphatidylcholine (1:1), PS:PE (1:1) or small unilamellar vesicles (SUV, 30 nm diameter) composed of PS, were determined. The vesicle concentration dependence of these rates, and the reversibility of the fluorescence signal with EDTA, were also examined. In all cases LM assays produced higher initial rates than the CM assay in the presence of the divalent cations, with the exception of SUV(PS) where LM and CM rates were similar in the presence of Ca^{2++}. The LMQ method resulted in significant aggregation-dependent RET between the probes. This was also observed for SUV(PS) aggregated with Na^{+}. The LMD method was not sensitive to liposome aggregation but in most cases showed higher initial rates of "fusion" than the CM assay. A variation of the LMD assay utilizing only 0.25 mol% of each probe (instead of the usual 1%), and a 1:1 mixture of labelled and unlabelled liposomes, resulted in initial rates of fusion most comparable to the CM assay. At present it is not possible to discriminate between lipid exchange, lipid transfer or the mixing of outer monolayers of liposomes in cases when the LM assays indicate fusion while the CM assay indicates no fusion.

T-AM-B2 PROTON-INDUCED FUSION OF LIPOSOMES AND THE INTRACELLULAR DELIVERY OF ENCAPSULATED MACROMOLECULES. N. Düzgüneş, R. M. Straubinger, P. A. Baldwin, D. S. Friend, and D. Papahadjopoulos, Cancer Research Institute and the Departments of Pharmacology and Pathology, University of California, San Francisco, CA 94143.

Liposomes composed of oleic acid (OA) and phosphatidylethanolamine (PE; 3:7 mol ratio) aggregate, become destabilized and fuse below pH 6.5 in 150 mM NaCl. Ca^{2+} and Mg^{2+} also induce fusion of these vesicles at 3 and 4 mM respectively. The threshold for fusion is at a higher pH in the presence of low (sub-fusogenic) concentrations of these divalent cations. Vesicles composed of phosphatidylserine (PS)/PE or of OA/phosphatidylcholine (PC; 3:7 mol ratio) do not aggregate,destabilize nor fuse in the pH range 7-4, indicating that both OA and PE are necessary components for proton-induced membrane fusion. Freeze-fracture replicas of OA/PE liposomes frozen within 1 sec of stimulation with pH 5.3 display larger vesicles and vesicles undergoing fusion, with membrane ridges and areas of bilayer continuity. Since negatively charged liposomes are endocytosed by the coated vesicle system and accumulate in acidic intracellular vesicles, OA:PE liposomes can be used to deliver encapsulated calcein (CAL) to the cytoplasm of CV-1 cells, as evidencedby the emergence of diffuse, cytoplasmic fluorescence. Delivery requires metabolic energy. With OA:PC or PS:PE liposomes, cells show only confined, vesicular fluorescence from CAL sequestered in intra- or extracellular vesicles. Glycerol treatment (5 min; 21% v/v) greatly enhances cytoplasmic delivery of CAL by OA:PE liposomes, and promotes delivery of large molecules such as FITC dextran (18k or 40k daltons) or SV40 DNA. (Supported by NIH grants GM28117, CA35340, HD10445; a Grant-in-Aid from the American Heart Association, and Fellowship PF-2331 from the American Cancer Society.)

T-AM-B3 DESTABILIZATION OF PHOSPHATIDYLETHANOLAMINE LIPOSOMES AT THE HEXAGONAL PHASE TRANSITION TEMPERATURE. H. Ellens, J. Bentz and F.C. Szoka, Departments of Pharmacy and Pharmaceutical Chemistry, School of Pharmacy, University of California, San Francisco, CA 94143.

We have examined the relationship between the lamellar-hexagonal phase transition temperature, T_H, and the initial kinetics of H^{+} and Ca^{2+} induced destabilization of PE liposomes. The liposomes were composed of dioleoylphosphatidylethanolamine (DOPE), egg phosphatidylethanolamine (EPE) or phosphatidylethanolamine, prepared from egg phosphatidylcholine by transesterification (TPE) because these lipids have well-spaced lamellar-hexagonal phase transition temperatures ($\sim 12°$, $\sim 45°$, $\sim 57°C$) in a temparature range that allows us to measure the initial kinetics of bilayer destabilization, both below and above T_H. The liposomes were prepared at pH 9.5. The T_H of EPE and TPE was measured using DSC and it was found that the T_H was essentially the same at low pH or at high pH in the presence of 20 mM Ca^{2+}. When incubated at pH 4.5 or at pH 9.5 in the presence of Ca^{2+} the liposomes aggregate, leak, undergo lipid mixing and mixing of contents. We show that liposome-liposome contact is involved in the destabilization of the PE liposomes. The temperature dependence of leakage, lipid mixing and mixing of contents shows that there is a massive enhancement of leakage, when the temperature approaches the T_H of the particular PE, that also lipid mixing is enhanced, but that the fusion (mixing of aqueous contents) is diminished or even abolished at temperatures above T_H. Thus, the polymorphism accessible to PE is a powerful agent for membrane destabilization but additional factors are required for fusion.
Supported by NIH grants GM-29514 (FCS) and GM-31506 (JB).

T-AM-B4 CONTACT INDUCED DESTABILIZATION OF PHOSPHATIDYLETHANOAMINE LIPOSOMES: EFFECT OF ASYMMETRIC BILAYERS. J. Bentz, H. Ellens and F.C. Szoka, Departments of Pharmacy and Pharmaceutical Chemistry, University of California, San Francisco, CA 94143.

We have shown for liposomes composed of pure PE and in mixtures with cholesterylhemisuccinate (CHEMS) that there is an interbilayer contact mediated destabilization which is greatly enhanced at and above the lamellar-H_{II} phase transition temperature T_H (Ellens et al., this volume). We now ask the question: how well can a DOPE/CHEMS liposome destabilize a TPE (transesterified from egg PC)/CHEMS liposome and vice versa. We used Ca^{2+} and H^+ to induce aggregation and to provide different values of T_H; the T_H of the PE/CHEMS mixture is much lower at low pH than with Ca^{2+}. The answer is quite clear, and most interesting. If the temperature is above the T_H of one lipid mixture, say A, and below the T_H of the other lipid mixture, say B, then the destabilization (measured by leakage kinetics) sequence is AA > AB >> BB. That is, the bilayer of the lipid A (which will end up in the H_{II} phase) destabilizes itself better than it destabilizes the bilayer of lipid B (which left on its own, remains in the lamellar phase). The BB contact is most stable. The surprising result is that if the temperature is either above the T_H or below the T_H of both lipid mixtures, then the destabilization sequence is AB > AA, BB. That is, the mixed bilayers are destabilized more by contact than either of the pure pairs. If inverted micelles (lipidic particles) are the mechanism of this destabilization, even below the equilibrium T_H, then one would conclude that "mixed micelles" destabilize more than "pure micelles." Research supported by NIH Grants GM-31506 (J.B.) and GM-29514 (F.C.S.).

T-AM-B5 DIVALENT CATION-INDUCED PHOSPHOLIPID MEMBRANE FUSION: EFFECT OF INTERFACIAL TENSION. S. Ohki and H. Ohshima. Dept. of Biophysical Sciences, State University of New York, Buffalo, NY 14214.

Divalent cation-induced acidic phospholipid (phosphatidylserine and phosphatidic acid) membrane fusion has been studied. The degree of these membrane fusions was correlated well with the increase in interfacial tension of the membranes induced by divalent cations. A theoretical explanation for the interfacial tension increase of acidic membranes by divalent cations is proposed.

Chelation binding of divalent cations to phospholipid membranes may cause deformation in the headgroup regions of these lipid molecules. This deformation may be responsible for the observed large increase in surface tension of acidic phospholipid membranes induced by divalent cations. On the other hand, simple binding of monovalent cations without being followed by such a deformation of membrane molecules, does not result in a large surface tension increase in the membrane. The divalent cation-induced acidic phospholipid membrane fusion as well as other lipid membrane fusions are discussed in terms of this increased surface energy of membranes.

T-AM-B6 FUSOGENIC CAPACITIES OF DIVALENT CATIONS: THE EFFECT OF LIPOSOME SIZE. J. Bentz[a] and N. Düzgüneş[b] (Intr. by M. R. Clark), [a]Departments of Pharmacy and Pharmaceutical Chemistry, and [b]Cancer Research Institute, University of California, San Francisco, CA 94143

The divalent cation (Ca^{2+}, Br^{2+}, Sr^{2+})-induced fusion of phosphatidylserine (PS) liposomes, LUV, is examined to obtain the fusion rate constants, f_{11}, as a function of bound divalent cation. The aggregation step is rendered very rapid by having Mg^{2+} in the electrolyte, so that the fusion step is rate limiting to the overall reaction. In this way the fusion kinetics are observed directly. The bound Mg^{2+}, which, by itself, is unable to induce the PS LUV to fuse, is shown to affect only the aggregation kinetics when the other divalent cations are present. There is a threshold amount of bound divalent cation below which the fusion rate constant f_{11} is small and above which it rapidly increases with bound divalent cation. These threshold amounts increase in the sequence $Ca^{2+}<Ba^{2+}<Sr^{2+}$, which is the same as found previously for sonicated PS liposomes, SUV. While Mg^{2+} cannot induce fusion of the LUV and much more bound Sr^{2+} is required to reach the fusion threshold for the LUV, for Ca^{2+} and Ba^{2+} the threshold is the same for PS SUV and LUV. The fusion rate constant for PS liposomes clearly depends upon the amount and identity of bound divalent cation and the size of the liposome. However, for Ca^{2+} and Ba^{2+}, this size dependence manifests itself only in the rate of increase of f_{11} with bound divalent cation, rather than in any greater intrinsic instability of the PS SUV.

(Supported by NIH grants GM31506 and GM28117, and a Grant-in-aid from the American Heart Association with funds contributed by the California Affiliate.)

T-AM-B7 IONOGENIC LATERAL PHASE SEPARATIONS AND FUSION OF VESICLES CONTAINING PHOSPHATIDIC ACID
Ian Graham, Jeannine Gagné and John R. Silvius, Department of Biochemistry, McGill University, Montréal, Québec, Canada H3G 1Y6

Calorimetric and fluorescence measurements have been correlated to ascertain the role of lipid lateral segregation in the divalent cation-induced fusion of vesicles containing phosphatidic acid (PA) alone or in combination with phosphatidylcholine (PC) or phosphatidylethanolamine (PE). Calorimetrically derived phase diagrams for the dielaidoyl and dimyristoyl PA-PC and PA-PE systems show good miscibility of these species in the absence of divalent cations, while high (mM) concentrations of calcium induce phase separation in bilayers containing ~10-80% PA in PC or ~5-80% PA in PE. Magnesium also promotes lateral segregation of PA from PC or PE, but to a lesser extent than does calcium. Measurements of the fluorescence of C_{12}-NBD-PA and -PC in dioleoyl or dielaidoyl PA-PC vesicles shows that calcium-induced phase separations are fast (sec. or faster), can occur without the establishment of interbilayer contacts, and most intriguingly, appear to proceed almost independently in the two halves of the bilayer when the calcium concentration is different at the two faces of the membrane. Parallel measurements of divalent cation-induced vesicle fusion suggest that the lateral segregation of PA-rich domains is important in the fusion of PA-PC vesicles but that other factors, notably vesicle size and internal osmotic pressure, are also of considerable importance in determining the tendency of the vesicles to fuse. These factors appear to be less crucial in determining the ability of vesicles containing PE to fuse under similar conditions. (Supported by the Medical Research Council of Canada).

T-AM-B8 CORRELATION OF FUSION ACTIVITY WITH PHYSICAL PROPERTIES OF FATTY ACIDS IN BILAYER MEMBRANES.
M. P. O'Brien and J. H. Prestegard, Department of Chemistry, Yale University, New Haven, CT 06511.

Fatty acids have been implicated in the stimulated fusion of both artificial and natural vesicles. Elucidation of the fusion mechanism depends both on the physical characterization of various fatty acids within a membrane environment and accurate determination of fusion activities. With an eye toward extending studies from artificial systems to natural granules, such as the chromaffin granule, we have investigated a fusion assay which relies on the presence of epinephrine in one fusion partner. The assay relies on a standard serological test in which epinephrine from one vesicle is oxidized and reacted with ethylene diamine from another vesicle to produce a fluorescent product. Conditions for rapid internal reaction and inhibition of reaction in external solutions are reported. Physical characterization of fusogenic fatty acids is pursued using solids ^{13}C NMR methods. Chemical shift anisotropy powder patterns are used to assess distribution between lipid phases and the time course of cross polarization is used as a probe of motion within and between phases. We hope that these parallel investigations of physical properties and fusion activities will lead to improved understanding of fusion mechanisms.

T-AM-B9 ELECTRIC FIELD - INDUCED MEMBRANE FUSION IN ERYTHROCYTE GHOSTS: EVIDENCE THAT PULSES INDUCE A LONG-LIVED FUSOGENIC STATE AND THAT FUSION MAY NOT INVOLVE PORE FORMATION.
Arthur E. Sowers, American Red Cross Laboratories, Bethesda, MD 20814.

Two or more membranes in suspension can be fused into one membrane by the application of a weak alternating current (AC) field followed by the application of one or more strong direct current (DC) pulses. Experiments from this laboratory (Sowers, 1984, J.C.B. 99, in press) using lipid-soluble and aqueous-soluble fluorescent labels, loaded into membranes or resealed cytoplasmic compartments, respectively, showed that the lumen diameter increase can be functionally separated from the fusion event by membrane dehydration with glycerol, and that application of fusion-inducing DC pulses first and then application of the AC treatment would also lead to fusion, thus showing that the membranes need not be in contact with each other for fusion to occur. New experiments show that a time interval of up to at least 2 - 3 minutes may be interposed between the DC pulses and the subsequent application of the AC to bring the membranes in contact with each other and still obtain fusion. Experiments in which DC pulse induced pore formation was followed by the loss of the aqueous label from the cytoplasmic compartment showed that fusion yields and pore formation are not correlated under certain conditions. Lastly, comparison of results from experiments using true square wave DC pulses and DC pulses having a square wave rise time and a fall time and a fall path which decays exponentically give qualitatively different fusion yields and behavior. These results suggest that precise collisions between opened pores on different membranes when the membranes are brought together would be improbable without invoking a more complicated mechanism.

T-AM-B10 MAST CELL EXOCYTOSIS AND THE GEL-SWELL OF GRANULES. M. Curran and M. S. Brodwick, Dept. Physiology and Biophysics, Univ. of Texas Medical Branch, Galveston, Texas 77550.

Our previous results suggest that granule osmolarity play a role in exocytosis. We have now shown that individual giant granules of Beige mouse mast (BMM) cells do contract in hypertonic stacchyose solutions. However, the contraction is less than predicted for a perfect spherical osmometer. The divergence of theory from measurement increases with hypertonicity. We find also that the ionophores, nystatin and gramicidin, cause granule lysis after one hour in highly permeabilized (nuclei stain with trypan blue) rat mast cells exposed to normal Ringer. Lysed BMM cell granules are about 20% larger than intact granules. Lysis was demonstrated by 0.005% ruthenium red staining. We noticed in BMM that as the lysed granule stained, it shrank. Other polyvalent cations also shrank the granule such as: polylysine, histamine, serotonin, ethylenediamine, Ca^{++}, Mg^{++}, decamethonium and hexamethonium. Certain monovalent cations did not cause shrinkage including: imidazole, lysine, histidine, tryptophan, and Na^{+}. Histidine, tryptophan, and 1 M NaCl, actually caused reversible granule expansion. ATP (124 mM) and pH in the range of 5.9-7.1 had no effect on the size of lysed vesicles. BMM cell granules expand 20% during exocytosis. When bathed in isotonic histamine Ringer or at pH 5.9 exocytosis induced by A23187 resulted in 10% granule expansion followed by a shrinkage back to its prereleased size. External 50 mM serotonin also caused contraction. Exocytosis was demonstrated by ruthenium red staining. We conclude that the granules are imperfectly osmotically active. The granule matrix is clearly capable of expansion and contraction in response to appropriate ionic constituents. Such gel-swell may aid in widening of the exocytotic orifice during secretion.

T-AM-B11 EFFECTS OF FREE FATTY ACIDS ON IN VITRO MODELS FOR EVENTS OCCURING DURING EXOCYTOSIS.

W.J. Zaks, D.C. Sterner and C.E. Creutz, Department of Pharmacology, University of Virginia, Charlottesville, Virginia 22908.

The aggregation and fusion of isolated chromaffin granules in the presence of Ca^{2+}, synexin, and cis-unsaturated fatty acids has been suggested as a model for events occuring during compound exocytosis. In an attempt to determine whether synexin-free fatty acid (FFA) interactions play a role in this process we have examined the effects of FFA on the ability of synexin to self-associate and promote phospholipid vesicle fusion. Ca^{2+}-dependent synexin polymerization was monitored by 350nm light scattering at 90°, while Ca^{2+}/synexin-dependent fusion of large unilamellar vesicles composed of PA/PE (1:3) was monitored by the Tb/dipicolinic acid fluorescence assay (Wilschut et al., Biochemistry 19, 6011 (1980)). Cis-unsaturated FFA, but not saturated FFA, or FFA methyl esters were found to potentiate both Ca^{2+}-dependent synexin polymerization and synexin-induced phospholipid vesicle fusion. Studies are in progress to determine whether FFA similarly affect calelectrin and polyamine induced liposome fusion. These results are discussed in terms of FFA modulation of lipid-protein interactions.

T-AM-B12 CAPACITANCE MEASUREMENTS CONFIRM HYPEROSMOTIC INHIBITION OF FUSION IN SEA URCHIN EGGS. J. Zimmerberg and M. J. Whitaker. Physical Sciences Laboratory, DCRT, National Institutes of Health, Bethesda, MD and Department of Physiology, University College, London, England

The driving force for exocytosis is obscure. Phospholipid vesicles must swell in order to fuse to planar phospholipid bilayers (Akabas, Cohen and Finkelstein, J. Cell Biol. 98:1063-1071). Is swelling a prerequisite for biological fusion? For many cells, hyperosmotic external media prevent secretion, as measured by release of contents. However, it has been an open question whether this inhibition was of actual membrane fusion or merely the dispersal of vesicle contents. We have measured the capacitance of sea urchin eggs during activation in hyperosmotic sea water to distinguish between these two possibilities.

The rapid and complete exocytosis of cortical vesicles in unfertilized eggs treated with a calcium ionophore is inhibited when the osmolality of the bathing sea water is raised from one to two Osm/kg, as judged by the continued presence of optically defined granules in differential interference contrast microscopy. This reversible inhibition, half-maximal at 1.7 Osm/kg, is quantitatively independent of choice of osmoticant - sucrose, stachyose, or sodium sulfate.

Upon ionophore treatment of eggs in sea water there is a large increase in membrane capacitance which is known to be due to the addition of cortical vesicle membrane upon fusion. In sea water made 2.4 Osm/kg with stachyose, only 4% of the control capacitance change is seen, although the full transient in conductance caused by calcium release is evident. These results are consistent with the idea that osmotic swelling of the secretory vesicle is a prerequisite for fusion.

T-AM-C1 PROGRESS IN THE 3-D STRUCTURE DETERMINATION OF Na/K-ATPase BY ELECTRON MICROSCOPY AND IMAGE PROCESSING. M. Mohraz and P.R. Smith. Dept. of Cell Biol. New York Univ. Sch. of Med. New York, NY 10016.

Na/K-ATPase is the Na, K pump found in the plasma membrane of most eukaryotic cells. It consists of two polypeptide chains; the catalytic subunit α (M_r = 100,000), and a glycoprotein subunit β (M_r = 50 - 60,000). The structure of the enzyme is being investigated by high resolution electron microscopy and image processing of its crystalline sheets. The studies of the structure of the enzyme in projection have led to the identification of the domains corresponding to its α and β subunits (J. Cell Biol. 1984. 98:1836). Work is in progress on the three dimensional reconstruction of the mass distribution from tilted views of the crystalline sheets of the enzyme. Tilt series have been recorded from the negatively stained arrays at tilt angles up to 60°. Preliminary results from the filtrations indicate that there is consistent recovery of high resolution information up to the maximum tilt, which should allow the computation of the structure to a resolution of at least 2.2nm. In order to extend the structural studies to higher resolution, attempts are being made to generate larger and better ordered arrays. The modification of the lipid environment of the enzyme has recently led to the formation of a new array type with a dimer of the molecule in the unit cell. The more regular features of this new crystal form as indicated by the higher resolution spots in its optical diffraction pattern, and the possibility of forming larger sheets render it very favourable for further structural studies. (Supported by grant GM-26723 to P.R.S).

T-AM-C2 STRUCTURE OF A GRAMICIDIN A/CESIUM COMPLEX. B.A. Wallace[1] and W.A. Hendrickson[1,2], [1]Department of Biochemistry & Molecular Biophysics, Columbia University, NY, NY 10032 and [2]Laboratory for Structure of Matter, Naval Research Laboratory, Washington, D.C. 20375

Gramicidin A, a linear polypeptide antibiotic, forms channels in phospholipid membranes which are specific for monovalent cations. Dimers of this hydrophobic molecule adopt very different conformations in membranes and in organic solvents, and different crystal forms have been prepared in the presence and absence of ions and/or lipid molecules [Wallace, Biopolymers 22, 397(1983)]. Crystals of one gramicidin/ion complex which diffract to 1.5 Å have been prepared from a CsCl solution in methanol [Kimball and Wallace, Ann. N.Y. Acad. Sci. (1984)]. This crystal form (space group $P2_12_12_1$, a=32.12, b=52.10, c=31.17 Å) contains 2 dimers per asymmetric unit. The Bijvoet differences from the 8 cesium sites per asymmetric unit were estimated to be 18% with a Cs^+ partial structure contribution of ~80% in F, so it was possible to calculate a 1.8 Å electron density map using single wavelength anomalous scattering for phasing. The average measured anomalous differences were ~8%. An atomic model has been fitted to the preliminary map and refinement of the structure is in progress. The dimer in this model is a left-handed double helix formed of two antiparallel β - strands wrapped into a helix with 5.6 residues per turn and with a helical repeat of 10.4 Å. The dimer is ~26 Å long with a central channel of ~4.4 Å diameter. Side chains are located axially on the perimeter of the channel. Two cesium sites are found in each channel at 7.1 Å from each end and are separated by 11.8 Å; two partially occupied cesium sites are also found between dimers in the crystal. There are also three strong features in each channel that appear to be chloride ions.

Supported by NSF Grant PCM 82-15109 to B.A.W. and NIH Grant GM-34102 to W.A.H.

T-AM-C3 CONFORMATIONAL STUDIES OF ALAMETHICIN IN LIPID VESICLES. M. Cascio and B.A. Wallace, Department of Biochemistry and Molecular Biophysics, Columbia University, NY, NY 10032

The secondary structure of alamethicin, a small membrane channel-forming linear polypeptide, has been examined by circular dichroism (CD) spectroscopy. The conformation of this molecule is very susceptible to influences of its environment. Its structure in a membrane system, small unilamellar dimyristoyl phosphatidylcholine (DMPC) vesicles, differs significantly from its structure in the organic solvents from which it has been crystallized (10% methanol/acetonitrile) (Fox and Richards [1982] Nature 300: 325) and examined by NMR spectroscopy (methanol) (Banerjee and Chan [1983] Biochem. 22: 3709). These results suggest that models previously proposed for the membrane-bound channel based on the structural data obtained in organic solvents may not be entirely appropriate.

CD spectroscopy has also been used to examine the effects of different methods of incorporation of the molecule into bilayers; it was found that the structure of alamethicin cosolubilized in DMPC vesicles was very similar to that of alamethicin added to preformed vesicles, though the latter method caused increased vesicle aggregation. Additionally, the effects of concentration (i.e., oligomerization) and the application of a transmembrane potential have been examined and both appear to also influence the secondary structure.

Supported by NSF grant PCM 82-15109 and NIH grant GM27292.

T-AM-C4 ENTRY MECHANISMS OF DIPHTHERIA TOXIN AND PSEUDOMONAS TOXIN. Leora Shaltiel Zalman and Bernadine J. Wisnieski (Intr. by Alfred F. Esser). Dept. of Microbiology and the Molecular Biology Institute, University of California, Los Angeles, CA 90024.

We have examined the membrane insertion and pore formation properties of two bacterial toxins: Pseudomonas toxin (PTx) and diphtheria toxin (DTx). Both toxins inhibit protein synthesis by ADP-ribosylating elongation factor 2. The photoreactive probe 12-(4-azido-2-nitrophenoxy)-stearoyl-1-^{14}C-glucosamine was used to monitor membrane insertion kinetics. Lipid vesicles were used as targets and samples were irradiated at 366nm for 15 sec at various times after toxin addition. Vesicles were floated through Ficoll step gradients to remove unbound toxin. Gel electrophoresis followed by protein staining and fluorography enabled us to distinguish between bound and inserted toxin (or fragment). Pore formation was established by a liposomal swelling assay. Binding, insertion and pore formation were examined as a function of time, temperature, pH, and extent of toxin cleavage with proteases. Low pH (~4) caused a dramatic increase in DTx and PTx binding and this was correlated with an increase in bilayer penetration. Only the cleaved form of DTx appeared capable of form formation (24Å diameter) but both cleaved and uncleaved DTx behaved identically in terms of membrane penetration. DTx fragments A and B were both photolabeled. PTx also formed large pores at pH 4. The temperature-dependent binding and insertion profiles of DTx and PTx indicated different abilities to penetrate frozen bilayers. Our results will be discussed in view of proposed entry models. Supported by USPHS GM22240, the UC Cancer Research Coordinating Committee, UCLA Academic Senate, the Calif. Inst. for Cancer Research CH830713 (LSZ) and the American Cancer Society (Inst. Grant IN-131; LSZ).

T-AM-C5 USE OF BROMINATED PHOSPHATIDYLCHOLINE TO INVESTIGATE THE TOPOGRAPHY OF CYTOCHROME B_5 Peter W. Holloway , Tom Markello, and Joan Tennyson. (Introduced by P.J. Sims) Dept. of Biochemistry, University of Virginia School of Medicine, Charlottesville, VA 22908.

The topography of cytochrome b_5 in lipid vesicles has been investigated by fluorescence quenching. The tryptophan fluorescence originating in the hydrophobic membrane-binding domain is quenched when the protein is incorporated into 1-palmitoyl-2-dibromostearoylphosphatidylcholine (BRPC). The bromine atoms were placed at different positions of the acyl chain, by bromination of the corresponding octadecenoic acid, and the quenching decreased along the series: 6,7- > 9,10- > 11,12- > 15,16BRPC. The lipid vesicles, prepared by sonication, had dimensions slightly larger than those of (1-palmitoyl-2-oleoyl PC) POPC as evidenced by trapped volume measurements whereas co-chromatography on Sephacryl indicated no difference in Stokes' radius of the 6,7BRPC, 15,16BRPC and POPC. The structures of the vesicles prepared from 6,7BRPC, 15,16BRPC and POPC were compared by measuring the accessibility of the tryptophan(s) of the cytochrome b_5 and of added diphenylhexatriene (DPH) to aqueous acrylamide. The quenching of the fluorescence (residual fluorescence in BRPC vesicles) of the DPH and of the tryptophan by acrylamide exhibited similar Stern Volmer plots in all three vesicle preparations (6,7BRPC, 15,16BRPC and POPC) which suggests that the structure of the three types of vesicles in their interface regions are similar. We interpret the quenching of cytochrome b_5 fluorescence by the different BRPC vesicles to indicate the tryptophan(s) quenched is (are) approximately 0.7 nm below the vesicle surface rather than near the center of the bilayer. Supported by GM 23858 and Training Grant GM 07267.

T-AM-C6 THE INTERACTION OF SMALL HYDROPHOBIC PEPTIDES WITH LIPID BILAYERS Russell E. Jacobs and Stephen H. White, Dept. of Physiology and Biophysics, University of California, Irvine, CA 92717

Most models for the insertion and translocation of proteins and polypeptides into and across membranes make specific assumptions about conformational and energetic changes associated with the transfer of the hydrophobic portions of proteins from water into the lipid bilayer. Thus, it is of fundamental importance to develop an understanding of how the hydrophobic portions of proteins interact with their surroundings. Toward this end, we are examining the interactions of tripeptides of the form P_n-Ala-R-Ala-O-t-Butyl with vesicles and liposomes. This study focuses on a systematic comparison of a series of hydrophobic peptides. Thus far we have measured water-bilayer partition coefficients for peptides with R = Gly, Phe, and Trp where P_n is the free amine. The partition coefficients for the Gly, Phe and Trp analogues are, respectively, 150, 950, and 4000. Moreover, upon mixing with lipid vesicles the Trp analogue experiences a greater than 300% increase in fluoresence intensity and a blue shift in emission maximum, indicating that the Trp side chain is intimately associated with the bilayer interior. Information concerning the extent of lipid perturbation induced by the peptides as measured by DSC thermograms of the mixtures and ^{2}H-NMR order parameters of ^{2}H labeled lipids will be presented. Research supported by NSF.

T-AM-C7 DISTRIBUTION OF CYTOCHROME b_5 BETWEEN SONICATED VESICLES OF DIFFERENT SIZE. Susan F. Greenhut and Mark A. Roseman, Department of Biochemistry, Uniformed Services University of the Health Sciences, 4301 Jones Bridge Road, Bethesda, MD 20814-4799

Cytochrome b_5 is an amphipathic integral membrane protein that spontaneously inserts, post-translationally, into intracellular membranes. When added to preformed phospholipid vesicles, it binds in a "loose" configuration, characterized by the ability of the protein to rapidly exchange between vesicles.

A heterogeneous dispersion of sonicated PC vesicles, about 220-400 Å in diameter, was prepared by differential centrifugation. When cytochrome b_5 was incubated with these vesicles (1 mol protein per 860 mol phospholipid, in 0.01 M $NaHCO_3$, 0.1 M NaCl, 10^{-4} M EDTA, pH 7.4), and the mixture subjected to molecular sieve chromatography on Sepharose 2B-CL, the cytochrome b_5 was found to elute preferentially with the smaller vesicles. Subsequently, a fresh preparation of heterogeneous vesicles was subfractionated by gel filtration, and the individual fractions incubated with the protein. Molecular sieve chromatography of these complexes shows that cytochrome b_5 favors the smallest over the largest vesicles by a factor of at least 20.

This result suggests that formation of highly curved regions in biological membranes may cause accumulation of certain membrane proteins at those sites.

Supported by NIH grant AM 30432 and USUHS Protocol G37138.

T-AM-C8 CONFORMATIONAL AND SURFACE PROPERTIES OF SYNTHETIC SIGNAL SEQUENCES. Martha S. Briggs[1,2] and Lila M. Gierasch[1], [1]Department of Chemistry, University of Delaware, Newark DE 19716, and [2]Department of Molecular Biophysics and Biochemistry, Yale University, New Haven CT 06511.

Secreted proteins are synthesized as precursors possessing a 15 to 30 residue amino terminal extension called a signal sequence. Although the signal sequence is required for protein translocation, its role in the process is unknown. An altered signal sequence can cause an export deficiency for its associated protein; thus, comparison of the properties of export-competent and export-deficient signal sequences may lead to insights into the mechanism of protein secretion.

We have synthesized wild type and mutant signal sequences of *E. coli* lambda receptor, an outer membrane protein. Preliminary circular dichroism data indicated that the ability to adopt an α-helical conformation correlates with an export-competent phenotype (Briggs & Gierasch, *Biochemistry 23*, 3111, 1984). The ability of the peptide to insert into phospholipid monolayers also correlates with *in vivo* function (Briggs, Gierasch, Lear, Zlotnick, & DeGrado, submitted). We report thermodynamic data calculated from the temperature dependence of the conformational transitions which occur upon changing the signal sequence's environment from aqueous to membrane-mimetic (e.g., trifluoroethanol or micellar detergent). In addition, the temperature dependence of the dissociation constant for insertion of the signal sequences into phospholipid monolayers was determined and used to calculate thermodynamic constants for the insertion process. The implications of these data for various models of protein secretion will be discussed. This work was supported by Grants GM27616 and GM29754 from the U.S. Public Health Service.

T-AM-C9 MUTATION OF THE ALKALINE PHOSPHATASE SIGNAL PEPTIDE. D.A. Kendall, S.C. Bock and E.T. Kaiser. Laboratory of Bioorganic Chemistry and Biochemistry, The Rockefeller University, New York, NY 10021

E. coli alkaline phosphatase is synthesized as a precursor with a 21 amino acid signal sequence. This signal peptide is necessary for transport of the enzyme to the periplasm. Translocation is mediated in part by the presence of a hydrophobic core in the signal sequence which, in this case, contains a proline at residue 12. We are investigating the possible role of an α-helical conformation in this region. Since proline would disrupt the conformational regularity of this proposed structure, we used oligonucleotide-directed site-specific mutagenesis to substitute this proline residue with leucine. Transport studies were conducted in an E. coli host containing a partial deletion of the alkaline phosphatase structural gene. The host strain was transformed with a multi-copy plasmid containing an alkaline phosphatase gene with a wild type or mutant ($pro^{12} \longrightarrow leu$) signal. These experiments show that the presence of the proline is not essential for alkaline phosphatase export. Processing of the precursor to the mature form, however, appears to be slower in the mutant than the wild type.

T-AM-C10 PHYSICAL AND CONFORMATIONAL PROPERTIES OF A SYNTHETIC LEADER PEPTIDE FROM M13 VIRUS COAT PROTEIN. Ann E. Shinnar and E. T. Kaiser, Laboratory of Bioorganic Chemistry and Biochemistry, The Rockefeller University, New York NY 10021

Leader peptide (lp) from M13 virus coat protein, Met-Lys-Lys-Ser-Leu-Val-Leu-Lys-Ala-Ser-Val-Ala-Val-Ala-Thr-Leu-Val-Pro-Met-Leu-Ser-Phe-Ala-NH_2, was synthesized by the Merrifield solid phase method on benzyhydralamine divinylbenzene resin and purified by reverse phase C18 HPLC using CH_3CN in phosphate buffer pH 2.7, containing sodium perchlorate. This lp is readily soluble in aqueous solution at acid and neutral pH and in organic solvents. Gel permeation chromatography indicates that the peptide exists in a monomer-dimer equilibrium in solution. The signal peptide is very surface active. M13 lp causes fusion of small unilamellar vesicles of egg lecithin. When spread in a Langmuir trough, this lp forms a stable monolayer, with a collapse pressure of 32 dynes/cm. The limiting molecular area A_∞ suggests the peptide forms a compact structure such as a helix at the air-water interface. Circular dichroism spectroscopy shows that the peptide is random coil in aqueous solution while in the presence of hexafluoroisopropanol, M13 lp becomes predominantly α-helical. These data support the hypothesis that leader peptides adopt some sort of helical structure in membranes.

T-AM-C11 MATURATION OF E. COLI ALKALINE PHOSPHATASE. J.F. Chlebowski and N. Parlet, Biochemistry Department, Virginia Commonwealth University, Richmond, Virginia 23298

Alkaline phosphatase, a dimeric Zn(II) metalloenzyme, is routinely isolated from strains of bacteria bearing a mutation in the pit 10 locus. When deprived of inorganic phosphate (P_i), such strains are derepressed for phosphatase biosynthesis which accumulates in the periplasmic space. As isolated under these conditions, the enzyme (the product of the pho A gene) exists as a mixture of "isozymes", differing by deletion of the amino-terminal Arg at none, one or both of the subunits. In contrast, enzyme isolated from log phase cells is a single species, previously characterized (on the basis of chromatographic mobility) as the asymmetric isozyme. Appearance of these species has been postulated to result from processive "stuttering". Isolation and characterization of these species indicates, however, that the initial product of biosynthesis and vectorial transport is invariant, having the "isozyme 1" sequence. Although apparently chemically identical, differences in surface charge (detected as alterations in chromatographic behavior) are observed which depend on the history of the biosynthetic system. A low molecular weight species is a co-isolate of such preparations which appears to influence the quaternary structure of the enzyme. As judged by the degree of protection against tryptic modification of the enzyme, this species may bind in the amino-terminal region of the protein. The data obtained indicates that active enzyme formed on proteolytic processing of the precursor sequence has the same primary structure in all growth conditions. Formation of the "isozyme" variants occurs only under conditions of induced biosynthesis and may be an adventitious consequence of the presence of a co-induced periplasmic exopeptidase. (Supported by Grant GM 27493 from the NIH)

T-AM-C12 AMPHIPHILIC β-STRAND PEPTIDES. D.G. Osterman, R. Mora, S.C. Meredith, and E.T. Kaiser. Laboratory of Bioorganic Chemistry and Biochemistry, The Rockefeller University, New York, NY 10021 and the Departments of Biochemistry, Chemistry and Pathology, University of Chicago, Chicago, IL 60637

In order to investigate the behavior of amphiphilic β-strand segments in proteins, we synthesized model peptides designed to exhibit this structure. The side chains in planar β-sheets formed by association of β-strands project alternately above and below the plane of the sheet. A sequence of alternating hydrophobic and hydrophilic amino acids will therefore be amphiphilic in a β-strand conformation. We synthesized two peptides having the sequence summarized as : (Val-Glu-Val-$(CF_3CO$-Orn$))_n$-Val, where n = 2 or 3. Treatment with 1M piperidine removes the trifluoroacetyl protecting group from the ornithines to provide the fully deprotected peptides. All the peptides exhibit a high degree of self-association, with the fully deprotected thirteen residue peptide 1 having a cooperative monomer-octamer equilibrium. The peptides also form very stable monolayers at the air-water interface, with collapse pressures in excess of 30 dynes for all four. Peptide 1 binds quite tightly to LDL, with a K_d measured at 1.45×10^{-7} M. The CD spectra of the peptides are indicative of mixtures of β-sheet and random coil conformations, with β-sheet contributions reaching nearly 80 % in aqueous solution.

T-AM-D1 UNDECAGOLD CLUSTER LABELING IN THE ELECTRON MICROSCOPIC ANALYSIS OF THE STRUCTURE OF NUCLEOPROTEINS. J. Varkey*, B. Stewart*, M. Beer*, H. Yang**, P. Frey**
*Department of Biophysics, Johns Hopkins University, Baltimore, MD 21218
**Institute of Enzyme Research, University of Wisconsin, Madison, WI 53705

The N-Hydroxysuccinimido (4 Carboxy) Phenylmaleimide derivative of undecagold cluster (Au_{11}-MBS) reacts specifically with SH groups of proteins. It is suitable as a label for electron microscopy because it is compact, dense and stable. It is detectable in TEM as well as in STEM. We are using it in various structural studies relevant to transcriptional control. λ repressor can be quantitatively converted to a form with one cluster per molecule. The modified and unmodified repressor has virtually the same affinity for the operator. In electron micrographs of the complex of DNA with the repressor, the clusters, indicating the bound proteins, are clearly visible. The 7S nucleoprotein complex of Xenopus (transcription factor III A with 5S RNA) has been labelled with Au_{11}-MBS: up to three clusters are bound per molecule of protein.

T-AM-D2 THE STRUCTURE OF RECA PROTEIN-DNA COMPLEXES AS DETERMINED BY IMAGE ANALYSIS OF ELECTRON MICROGRAPHS. E. Egelman, A. Stasiak, S. West, and P. Howard-Flanders
Dept. of Mol. Biophysics and Biochem., Dept. of Therapeutic Radiology, Yale University, New Haven, Ct. 06511; Institute for Cell Biology, E.T.H., Zurich, Switzerland.

The recA protein is responsible for general genetic recombination in E. coli. In vitro, it forms a helical polymer which can contain either single or double stranded DNA. The activities of the recA polymer, including searching for homology among different DNA molecules as well as promoting the strand exchange reaction, are dependent upon an ATP-ase activity. We have examined the structure of two different conformations of the recA polymer: in the absence of nucleotide co-factors, and in the presence of a non-hydrolyzable ATP analog, ATP-gamma-S. With ATP-gamma-S, the recA polymer is a very "open" structure characterized by a deep groove along a 95Å pitch right-handed helix which links every subunit. We find an average of about 6.2 recA monomers per turn of this helix, in agreement with the value of Di Capua et al. (JMB 157, 87). The deep helical groove allows the structure to be easily extended and compressed. In the absence of nucleotide co-factors the 95Å pitch helix is reduced to a 64Å pitch helix, the deep helical groove disappears, and the mass per unit length of the filament increases by over 200%. Every monomer in this state is no longer equivalent, and the asymmetric unit appears to consist of three recA monomers. The implications of these structural studies for the role of recA protein in recombination will be discussed.

T-AM-D3 STRUCTURAL STUDIES OF THE LAMBDA REPRESSOR HEAD-PIECE FRAGMENT (RESIDUES 1 TO 102) BY RAMAN SPECTROSCOPY. B. Prescott, A. Nilsson, M. Weiss and G.J. Thomas, Jr., Department of Chemistry, Southeastern Massachusetts University, North Dartmouth, MA 02747

Raman spectroscopy has been employed to investigate structural characteristics of the "head-piece" fragment (residues 1 through 102) of phage lambda cI repressor. Studies have been carried out over the same range of protein concentration (5 to 100 mg/ml) for which NMR data indicate progressive formation of a head-piece dimer (M. Weiss et al., unpublished results). Significant changes in the Raman spectrum as a function of protein concentration have been detected and assigned to specific molecular subgroups which undergo changes in conformation or state of hydrogen bonding. The major findings are: (1) The hydroxyl group of each of five tyrosine residues in the monomer (5 mg/ml) acts as both donor and acceptor of moderately strong hydrogen bonds. Tyrosines are presumably on the surface of the monomer and/or accessible to solvent. (2) In the dimer (100 mg/ml), at least one and possibly two of the tyrosines are altered, such that each corresponding hydroxyl group acts solely as acceptor of a strong hydrogen bond from an as yet unidentified highly positive donor group. Y_{85} and Y_{88} are suggested as the altered tyrosines. (3) Dimerization causes little change in the backbone structure, in the direction of slightly more alpha-helix for the dimer than for the monomer. (4) The average environment of the two phenylalanine rings, F_{51} and F_{76}, differs in the monomer and dimer states. Raman studies of repressor sequence containing 2,6- and 3,5-dideuteriotyrosines confirm the above findings.

Supported by N.I.H. Grants AI11855 (G.J.T.) and AI16892 (R.T. Sauer, M.I.T.).

T-AM-D4 CO-CRYSTALS OF DNA AND A DNA BINDING PROTEIN S. R. Jordan, T. V. Whitcombe and C. O. Pabo, Laboratory of Molecular Structure and Function, Department of Biophysics, Johns Hopkins Medical School, Baltimore, Md., 21205.

The three dimensional structure of several site specific DNA binding proteins have been determined in the past several years. This structural information in combination with chemical, biochemical and genetic studies has led to models of the protein-DNA complexes. To test the models, we have grown diffraction quality crystals of a complex between the amino terminal domain of the lambda repressor and a synthetic fragment of DNA containing the full 17 base pair lambda repressor binding site. The lengths of the DNA segment were found to be critical for obtaining suitable crystals. We tested DNA segments ranging from 17 to 23 base pairs in length, and found the best crystals were grown with a 20 base pair length. The crystals diffract to a resolution of 3 Angstroms. The space group of the crystals is P21, with unit cell parameters a=37.5; b=69.4; c=57.5 and β=91.7. From the dimensions of the unit cell we calculate the asymmetric unit of the crystal to contain one protein-DNA complex. The complex is composed of the 20 base pair DNA duplex and a dimer of the amino terminal domain of lambda repressor. From packing constraints of the unit cell and from examining the diffraction pattern which shows the direction of the DNA in the crystal, a tentative model of the orientation of the complex in the crystal has been made.

T-AM-D5 NMR STUDIES OF THE EFFECT OF TEMPLATE ON THE CONFORMATION OF ATP BOUND TO E. COLI RNA POLYMERASE. R.P. Pillai, E. Tarien, G.A. Elgavish and G.L. Eichhorn, National Institutes of Health, Gerontology Research Center, Baltimore, Maryland 21224.

During RNA synthesis substrate molecules for E. coli RNA polymerase are selected on the basis of Watson-Crick complementarity with bases on the DNA template. It might therefore be expected that the template influences the conformation of the substrate. To test this possibility the paramagnetic effects of Mn(II) on the NMR relaxation rates of ATP substrate were studied in the presence of the enzyme with and without template, and the distances calculated from the enzyme-bound Mn(II) to the H-8, H-2 and H-1' protons and the P_α , P_β and P_γ phosphorus nuclei of ATP. The results indicate that the conformation of ATP bound to the enzyme is not perturbed by the presence of poly(dA-dT)·poly(dA-dT). This conclusion is in line with predictions by Koren, Bean and Mildvan [Biochemistry 16, 3322-3333 (1977)].

T-AM-D6 EPR STUDIES ON THE ACTIVE SITE OF RNA POLYMERASE. Peter P. Chuknyiski, Joseph M. Rifkind and Gunther L. Eichhorn, National Institutes of Health, Gerontology Research Center, Baltimore, Maryland 21224.

The metal atoms at the active site of RNA polymerase can serve to probe the structure of the active site. NMR has been used to study the effects of paramagnetic metals at the initiation site [Chatterji, Wu and Wu: J. Biol. Chem. 259, 284-289 (1984)] and the elongation site [Bean, Koren and Mildvan: Biochemistry 16, 3322-3333 (1977)]. We now study the effects of the metals on each other. The intrinsic Zn located in the initiation site of the β subunit of Escherichia coli RNA polymerase was substituted in vitro by the paramagnetic ion Mn(II). It was shown that the EPR spectrum of the substituted Mn(II) at temperature 80°K differs significantly from the spectrum of free manganese ion in frozen solution and from the spectrum of extrinsic Mn(II) bound to the elongation site of the β subunit. The perturbation of the EPR spectra when external Mn(II) is added to manganese substituted enzyme permits estimation of the distance between the two manganese ions to be 5 Å. This finding is in line with other studies that suggest close proximity of the elongation and initiation sites, and also with the spatial requirements of the active site. Further studies are underway to characterize the active site relationships.

T-AM-D7 DYNAMICS AND ORGANIZATION OF NUCLEOSIDES IN SINGLE STRANDED NUCLEIC ACID - POLY-L-LYSINE COMPLEXES. S-C. Kao, E. V. Bobst, and A. M. Bobst, Department of Chemistry, University of Cincinnati, Cincinnati, Ohio 45221

Site-specifically spin labeled nucleic acid bases substituted in position 4 or 5 with spin labels were incorporated enzymatically into single stranded homopolymers. The spin labeled - to unlabeled nucleotide ratio varied from 0.01 to 0.12 and the average molecular weight of the spin labeled homopolymers was 100,000. The spin labeled nucleic acids were complexed with stoichiometric amounts of poly-L-lysine with an average molecular weight of 41,000. Electron spin resonance (ESR) spectroscopy was used to monitor the ESR lineshape changes of the spin label as a result of complexation. A theorectical analysis of these lineshapes and intensities displays the presence of two distinct sets of spin labeled nucleosides in the complex, each representing mobile or immobilized spin labeled nucleosides. The population of mobile spin nucleosides in the complex is 25 to 35% and was found to be independent of the amount of spins incorporated in the nucleic acid lattice. Based on a model described earlier (J. Mol. Biol. 173, 63-74 (1984)) to analyze ESR data of mobile spin labeled nucleosides, the correlation time reflects the motion of the base. This motion was determined to be on the order of 8 ns which is by about a factor 7 larger than found in the uncomplexed polynucleotides. Based on these data we propose that a single stranded nucleic acid - poly-L-lysine complex is organized in strongly immobilized (on an ESR time scale) oligomer segments of 2 to 4 nucleosides which are flanked by mobile nucleosides with a base mobility of about 8 ns. (Supported in part by NIH grant GM-27002.)

T-AM-D8 INCREASE OF THE STRAND EXCHANGE ACTIVITY OF RecA PROTEIN BY REMOVAL OF THE C-TERMINUS AND STRUCTURE-FUNCTION STUDIES OF THE RESULTING FRAGMENT
Robert C. Benedict and Stephen C. Kowalczykowski. (Inro. by Peggy J. Arps)

A proteolytic fragment of recA protein, missing about 15 percent of the C-terminus, was found to promote exchange of homologous single-stranded DNA into duplex DNA more efficiently than intact recA protein. This difference was not found if single-stranded binding protein(SSB) was present. ATPase activities for recA protein and the fragment were identical. The fragment was found to bind double-stranded DNA more tightly and to aggregate more than recA protein. Both properties are probably important in strand exchange. The double-stranded DNA binding of both recA protein and the fragment responds to nucleotide cofactors in the same manner as single-stranded binding, i.e. ADP weakens and ATP-γ-S strengthens the association. The missing C-terminal region includes a very acidic portion that is homologous to other single-stranded DNA binding proteins, and has been shown to modulate DNA binding. This region appears to have a very similar function in the case of recA protein, possibly preventing destabilization of duplex DNA. The results suggest a single DNA binding site for both single-stranded and double-stranded DNA.

T-AM-D9 FREE ENERGY TRANSDUCTION IN GYRASE. Hans V. Westerhoff and Yi-der Chen, Laboratory of Molecular Biology, NIADDK, NIH, Bethesda, MD 20205

DNA gyrase is a biological free energy transducer with distinct properties. This procaryotic type II topoisomerase [1] hydrolyzes ATP and puts negative supercoils into circular DNA. This hydrolytic free energy, corresponding to the intracellular phosphate potential ($\Delta G_p = \Delta G_p^\circ + RT\ln[ATP]/([ADP].[P_i])$) is transformed to elastic energy of superhelical DNA[2]. The ATPase and supercoiling activities of gyrase are not strictly coupled; the enzyme exhibits 'molecular slip'[3,4].

One way to characterize free energy transducers is to compare the maximum output free energy they can generate at different magnitudes of the input free energy. Along this line we have examined in vitro how the extent of supercoiling of circular DNA varies with the concentration ratio of [ATP] and [ADP].

1. Gellert,M.(1981) Annu. Rev. Biochem. 50, 879-910.
2. Benham, C. J. (1980) J. Chem. Phys. 72, 3633-3639.
3. Pietrobon, D., Azzone, G. F. and Walz, D. (1981) Eur. J. Biochem. 117, 389-394.
4. Westerhoff, H. V. and Dancsházy, Z. S. (1984) Trends. Biochem. Sci. 9, 112-116.

T-AM-D10 A COMPARISON OF SOME SMALL HISTONE-LIKE PROTEINS WITH LINKER HISTONE AND HMG PROTEINS IN CHROMATIN RECONSTITUTION STUDY. D.C. Chan, P.D. Harney, J. Oide, M. Tanaka and L.H. Piette. Cancer Research Center of Hawaii, University of Hawaii, Honolulu, Hawaii 96813.

Three small chromosomal proteins have been isolated from the nuclei of chicken erythrocyte. These proteins are very lysine-rich and do not contain any acidic or aromatic residues. Their apparent molecular weights are found to be about 7000 to 8000. Amino acid analysis and immunoblotting studies suggest that they are not the degraded products of histone H1, H5 or the four core histones. We have examined their possible role involved in the chromatin structure by allowing them to reassociate with stripped chromatin (non-histone proteins and linker histones H1, H5 depleted). The reconstituted complexes were analyzed by nuclease digestion, thermal denaturation and sedimentation, and were compared to those complexes reconstituted with purified histone H1 and H5 or with purified HMG1, 2, 14 and 17 respectively. We found that these three histone-like proteins can effectively cause chromatin aggregations like those linker histone H1 and H5 do in the solubility study. When the reconstituted complexes were centrifuged through a 10% to 40% sucrose gradient containing 80mM NaCl, we found that about 1.2 molecule of these proteins per nucleosome is as effective as two molecules of H1 or H5 on condensing the chromatin higher-order structure; while the HMG proteins do not affect the chromatin condensation at all. We have used several gel electrophoresis systems to examine the micrococcal nuclease digest products of the reconstituted complexes, and found that these histone-like proteins do not protect the linker DNA from the nuclease digestion. These proteins remain bound to the nucleosome core particle even after extensive nuclease digestion. Our data suggest that these histone-like proteins are a group of unique proteins that share some properties between histone H1 and HMG14 (or 17) and they may play a role on higher-order chromatin organization.

T-AM-E1 LOCATION AND EVALUATION OF PROTEIN DOMAINS.
Micheal H. Zehfus and George D. Rose, Department of Biological Chemistry, Pennsylvania State University, Hershey Medical Center, Hershey PA 17033.

A parameter called the surface coefficient is derived which compares the accessible surface area of a contiguous protein segment the area it would have if perfectly packed into a sphere. This normalized parameter, a sensitive measure of local compactness and globularity, is applied to 20 proteins to find locally compact structures. The compact units found in this manner are intuitively satisfying and compare favorably with many domains found by other methodologies. A listing of these domains is presented, and some implications of these units for protein taxonomy and folding are addressed. These include the location of small highly compact regions which contain neither helices nor sheets, but only loops and turns, and the modeling of some hypothetical folding pathways based on the hierarchical growth of closely related compact units.

T-AM-E2 EVOLUTIONARY SIMILARITY AMONG PEPTIDE SEGMENTS IS A BASIS FOR PREDICTION OF PROTEIN FOLDING. Robert M. Sweet (Intr. by F. William Studier) Brookhaven National Laboratory, Upton, NY 11973

Short segments of polypeptide, from a protein for which the primary sequence but not the three-dimensional structure is known, are compared to a library of known structures. The basis of comparison is the odds with which residues in the unknown segment might have been substituted through evolution for residues in segments from the library of known structures. Segments from known structures that are similar in sequence to those from the unknown protein are often found to be similar in three-dimensional structure to one another and to the true structure of the segment from the unknown protein. This provides a basis for prediction not only of secondary structure type, but also of actual three-dimensional structure.

T-AM-E3 **DOMAIN UNFOLDING OF INTACT APO THERMOLYSIN.** RONALD J.T. CORBETT and RODNEY S. ROCHE (Intr. by A.L. Jacobson), Biochemistry Division, Department of Chemistry, The University of Calgary, Calgary, Alta., Canada, T2N 1N4.

We have examined the domain folding hypothesis for the case of the two domain metalloendopeptidase thermolysin. A stable species of metal free apothermolysin was prepared by successive incubations in phenanthroline and EDTA, followed by passage down a Sephadex G-15 column. Urea and guanidinium hydrochloride induced unfolding of apothermolysin was studied using a variety of spectroscopic techniques (CD, UV, fluorescence) as well as size exclusion chromatography. Biphasic unfolding transitions were observed in the presence of either denaturant, implying that apothermolysin possesses two independent unfolding domains. The magnitude of the transistions observed are consistent with the notion of the unfolding of an N-terminal domain (ΔG_N = 1 kcal/mole) at low denaturant concentrations (less than 2 M), followed by unfolding of a C-terminal domain (ΔG_C = 4 kcal/mole) at higher denaturant concentrations.

Our proposed domain unfolding pathway is consistent with the molecular weight distribution of autolytic and tryptic fragments produced from apothermolysin. Proteolysis results in the production of fragments with molecular weights of 21 kD (residues 1 to 200-210) and 12 kD (residues 200-210 to 316). These fragments showed differential stability towards further tryptic cleavage when incubated at intermediate concentrations of urea. For instance, in 2 M urea, the N-terminal fragment is rapidly cleaved to low molecular weight peptides while the C-terminal fragment remains intact.

Calcium saturated thermolysin is more resistant to urea or guanidinium hydrochloride induced unfolding. Also, in the presence of bound calcium or terbium, the rate of autolytic or tryptic cleavage of thermolysin is greatly reduced. The latter results suggest that metal ions bound at sites 1, 2, or 4 serve to act as an interdomain lock, protecting an interdomain region which is sensitive to unfolding or proteolysis. Supported by NSERC-A3608 (RSR) and AHFMR (RJTC).

T-AM-E4 MUTAGENESIS AS A PROBE OF ENZYME STABILITY AND ACTIVITY. C. R. Matthews, J.-T. Chen, K. M. Perry, M. H. Matthews, P. A. Benkovic and S. J. Benkovic, Department of Chemistry, and T. Yaegashi, M. E. Nemeroff and C.-P. D. Tu, Department of Biochemistry, Microbiology, Molecular and Cell Biology, The Pennsylvania State University, University Park, PA 16802.

The effect of replacing Glu 139 with Lys on the stability and activity of dihydrofolate reductase from Escherichia coli was studied. Glu 139 participates in a hydrogen-bonded salt bridge with His 141 which is remote from the active site and allows a test of the role of the protein matrix in the activity of this enzyme. The Glu 139 → Lys mutant protein is significantly less stable than the parent protein at pH 7.8: the midpoint for the urea-induced unfolding decreases from 3.3 M to 2.5 M urea and the melting temperature decreases from 47°C to 36°C. Noncoincidence of difference UV and far UV circular dichroism transition curves for both urea and thermal unfolding shows that both processes involve stable intermediates. The activities of the parent and mutant proteins are the same both at 15°C, below the thermal transition, and at 40°C where the parent protein and mutant proteins are 5% and 67% unfolded, respectively. These results suggest that the thermal unfolding process populates intermediates that retain catalytic activity.

This work was supported by NSF grant PCM-81-04495 (CRM) and by PHS grants GM13306 (SJB) and KO4 AG00153 (CRM).

T-AM-E5 SPECIES AND TISSUE COMPARISONS OF THE AMINO ACID SEQUENCE OF THE ATP BINDING SITES OF (Na,K)-ATPase AND Ca-ATPase. T.L. Kirley, E.T. Wallick, T. Wang, and L.K. Lane, Dept. of Pharmacology and Cell Biophysics, Univ. of Cincinnati, Cincinnati, Ohio 45267-0575

Fluorescein 5-isothiocyanate (FITC) covalently labels the 100 KDa component of ATPases, presumably at the ATP binding site, and inactivates them. A mixture of peptides containing the labeled lysine residue can be released from membrane bound enzyme by trypsin digestion, and the FITC-containing peptide can be purified by reversed phase HPLC, using trifluoroacetic acid as an ion pairing reagent and a gradient of water and acetonitrile. The pure, labeled peptides are characterized by isoelectric focusing and SDS-page, and sequenced in a gas phase sequenator. For lamb and rat kidney (Na,K)-ATPase the peptide obtained has a pI of 5.3 and a sequence of His-Leu-Leu-Val-Met-Lys*-Gly-Ala-Pro-Glu-Arg, showing complete homology between a ouabain sensitive (lamb) and ouabain insensitive (rat) species.

Ca ATPases from various sources were also examined and found to have homologous but different sequences from (Na,K)-ATPases. Ca ATPase from rabbit skeletal muscle yields 2 FITC peptides, one of which is 4 residues longer than the other. The pIs of the two peptides are 4.5 and 5.0 for the shorter and longer peptides, respectively. The sequences obtained are: Met-Phe-Val-Lys*-Gly-Ala-Pro-Glu-Gly-Val-Ile-Asp-Lys-(Leu-Asn-Tyr-Val). These results explain and confirm the results of Mitchinson et al. (FEBS Lett. 146, 87-92, 1982). Identical results are obtained for dog skeletal muscle Ca ATPase. These results are being compared to those obtained with dog heart (Na,K)-ATPase and Ca ATPase. In summary, there appears to be extensive conservation of the putative ATP binding site across both species and tissue lines, but less homology between different enzyme types.
Supported by T32 HL07382, PO1 HL22619 and RO1 HL25545.

T-AM-E6 A STRATEGY FOR THE DESIGN OF SYNTHETIC REPRESSOR MOLECULES
Allen T. Ansevin, Department of Physics, University of Texas System Cancer Center, Texas Medical Center, Houston, Texas 77030.

The insight gained from recent studies of repressor proteins supports a proposal that synthetic repressors might eventually be designed for interaction with specific segments of double stranded DNA. A theoretical evaluation (A.T. Ansevin, Biophys. J. 41, 401a, 1984) indicates that no simple code exists to govern specific protein-DNA interactions and that the directional features of H-bonds and the three-dimensional contours of complementary surfaces are critical for sequence specificity.

A computer program has been designed to select favorable residues in an 11-residue alpha helix, such that a maximum number of bidentate H-bonds can be formed by association with any specified DNA sequence of 11-base pairs in standard B-form geometry. The program takes advantage of geometric restrictions observed on space-filling models. It is concluded that the designing task is facilitated by the inclusion of an amino acid couple, such as SER:GLN, ASP:ARG, etc., at the start of the residue selection process.

Future experimental work is planned to test the merits of the current design strategy by comparing binding constants for synthesized peptides having sequences predicted by the program to those with variants of the given sequence.

T-AM-E7 CRYSTAL ENERGY MINIMIZATION OF CRAMBIN: AN ANALYSIS OF HYDROGEN BONDING. M.M. Teeter and M. Whitlow (Department of Chemistry, Boston University, Boston, Ma. 02215 USA) and B. Brooks and M. Karplus, (Dept. of Chemistry, Harvard Univ., Oxford St., Cambridge, Ma., 02139, USA.)

Crambin is a small, hydrophobic plant protein (MW = 4700) with no known function. However, crystals of it diffract to 0.88 A (Teeter and Hendrickson, J. Mol. Biol. (1979) 127, 219-224). The model obtained from the structure solution and refinement at 1.5A (Hendrickson and Teeter (1981) Nature 290, 107-113) has been refined against the 0.945 A data by restrained least squares techniques (Hendrickson and Teeter, unpublished).

The detailed geometry of crambin (bond lengths and angles, dihedral and planarity) will be described and compared with peptide geometry from analysis of the Cambridge Crystallographic Data File and from other models currently in use. Features of the secondary structure (hydrogen bonding patterns and distortions from ideal geometry) will be discussed.

This model, which includes 64 of the expected 85 water molecules in the crystal, has been subjected to full-crystal, potential energy minimization using the program CHARMM. Different hydrogen-bonding potential energy functions have been tested and compared with the crystallographic results. Structural criterea, such as the detailed hydrogen bonding distances and the number of hydrogen bonds made to the protein and to water, are used to evaluate the models.

T-AM-E8 PRELIMINARY CRYSTALLOGRAPHIC DATA FOR A THERMOSTABLE FORM OF BOVINE RIBONUCLEASE A Patricia C. Weber (Introduced by D. H. Ohlendorf), Protein Engineering Division, Genex Corporation, 16020 Industrial Drive, Gaithersburg, Maryland 20877 Chemically modified proteins have served as the basis for many biochemical studies. In the interpretation of the experimental results, it is generally assumed that the native protein conformation is essentially preserved and may only be altered in the local region of the modification.

Recently, the thermodynamic properties of a chemically cross-linked derivative of ribonuclease A have been reported (Lin, S.H., Konishi, Y., Denton, M.E., and Scheraga, H.A. (1984) Biochemistry, in press). Reaction of 1,5-difluoro-2,4-dinitrobenze with bovine pancreatic ribonuclease A resulted in the introduction of a cross-link between lysine residues 7 and 41. Refolding experiments reversible show a thermal transition at a temperature 25 degrees C higher than native ribonuclease A. The observed increase in thermal stability has been attributed to a loss in entropy of the protein in its unfolded state. In order to test the assumption that the native conformation is unaltered by the cross-linking reagent, we have initiated structural studies of the cross-linked form of ribonuclease A.

Crystals have been grown by dialysis against 30% (v/v) ethanol: water mixtures buffered at high pH. Single crystals belong to the orthorhombic space group $P2_12_12_1$ a = 37.1A, b = 41.2A, c = 75.6A, with one molecule in the crystallographic asymmetric unit. Crystals are quite stable at room temperature in the x-ray beam, and an initial three dimensional set of diffraction intensities to 2.1A resolution has been collected. Attempts to solve the structure by molecular replacement methods using the refined structure of ribonuclease A as a starting model will be discussed.

T-AM-E9 A FAST MOLECULAR MECHANICS COMPUTING DEVICE. C. Levinthal, R. Fine, and G. Dimmler, Columbia University and Brookhaven National Lab.

Computing power sufficient to investigate protein structure by searches for global energy minima has for the most part been unavailable to the scientific community. The same is true of molecular dynamics simulations for biologically meaningful periods of time and full Monte Carlo techniques including equilibration of solvent. To achieve significantly greater computing power we have designed and are building a hard-wired, long pipeline device Fastrun (FR) which will calculate and accumulate the vector force on each atom due to pairwise central interactions between all atoms. Our device passes the force vectors and the total energy to a commercial array process (AP) which can be programmed to calculate the required changes in coordinates at each step. Calculations in FR are done using commercially available 32 bit floating point adders and multipliers, with 64 bit accumulation. All forces between atom pairs are obtained by table look-ups using quadratic interpolation. Fast memories are used to store functional values and first and second derivatives. All of these values are loaded and can be changed by the host computer. Pair-lists are first loaded by the host and subsequently updated by the AP, and all necessary 3 and 4 body interactions' are calculated in the AP.

The speed of this system will allow one pairwise interaction to be calculated in the pipeline in FR every 100 ns. The overall speed is about a thousand fold greater than that available from a VAX 11/780 and about 10-25 times faster than a Cray 1S. Although this speed can only be used for molecular mechanics, we believe that it can handle most versions of molecular mechanics algorithms which are likely to be used during the next decade.

T-AM-E10 PROTEIN STRUCTURE DISPLAY USING GRAPHICS FOR ENGINEERING ANALYSIS. J.W. Duane and E.L. Gross, Depts. of Engineering Graphics and Biochemistry, The Ohio State University, Columbus, Ohio, 43210.

By adapting local engineering graphics software, we were able to display any molecules whose coordinates are available from the Brookhaven Protein Data Bank without having to install a dedicated molecular graphics system. The program that was used is General Electric CAE International's I-DEAS package. The software is available at many universities through SDRC's Universities Program. The software runs on a variety of minicomputers and can be displayed on inexpensive raster color terminals. By writing a preprocessor, we were able to adapt the I-DEAS package to display the molecular coordinates of macromolecules obtained from the Brookhaven Data Bank. Both wire-frame and solid models can be displayed. Individual residues are coded in different colors. Models can be rotated, displayed in perspective and sliced for interior viewing. The capabilities of the program will be demonstrated using the electron transport protein plastocyanin. This software allows investigators to gain insights into molecular structure and function without needing extensive computer expertise or access to a dedicated molecular graphics system.

T-AM-F1 Photoaffinity Labelling of Gizzard Myosin with 3'-O(4-benzoyl)benzoic Adenosine Triphosphate (BzATP). Sudhir Srivastava, Michael B. Cable, and Stephen P. Driska, Dept. of Physiology and Biophysics, Medical College of Virginia, Richmond, VA. 23298.

[α-^{32}P]BzATP, synthesized from [α-^{32}P]ATP (J. Biol. Chem. 257,2834-2844,1982), was photoincorporated into gizzard myosin (4-5 mg myosin/ml in 0.5 M KCl and 0.2 M DTT) at 0-4°C for 10 min in a Pyrex cuvette with a long-wavelength UV lamp at BzATP concentrations in 5-10 fold molar excess over myosin. Both the K(EDTA)ATPase and the Ca-ATPase activities of myosin were inhibited compared to illuminated controls. Mg-activated and Actin-activated ATPase activities were unaffected while the inhibition due to the light alone was never more than 10%. The inhibition was linear with the amount of [α-^{32}P]BzATP incorporated. The maximum inhibition obtained at high BzATP concentrations was 70% which was produced by 1.1 mol BzATP incorporated per mol myosin head. BzATP was a substrate for myosin ATPase, although the rate of hydrolysis was low compared to ATP. In order to localize the label in myosin heavy chain S1 (prepared using papain) was labeled with BzATP and subjected to tryptic digestion. Before digestion, the S1 contained two heavy chain fragments (94K and 76K) and the 20K light chain. Radioactivity was chiefly incorporated into the 94K and 76K peptides and to a minor extent in the 20K peptide. During tryptic digestion, the 94K peptide was converted into a labelled 76K peptide, and this peptide was then digested into 50K, 29K, and 28K peptides, all containing label. A 25K peptide with a small amount of label was also produced. Although present studies suggest that the 28K peptide participates in the active site, further studies are in progress to see if the 25K peptide also contributes to the active site.

T-AM-F2 PHOSPHORYLATION DEPENDENT 7.5S-9S TRANSITION OF GIZZARD HEAVY MEROMYOSIN (HMM): ELECTRON MICROSCOPIC, SEDIMENTATION AND BIOCHEMICAL OBSERVATIONS, H. Suzuki*, W.F. Stafford, III.*, H.F. Slayter+, and J.C. Seidel*, *Dept. Muscle Res., Boston Biomed. Res. Inst. and +Dana-Farber Cancer Res. Inst. Boston, MA

Gizzard myosin can exist in two conformational states having sedimentation coefficients (S20,w) of 6S and 10S. HMM undergoes a similar transformation sedimenting at 7.5S in 0.3 M NaCl and at 9S in 20 mM NaCl, i.e. S20,w increases below 0.3 M NaCl (Suzuki et al., 1982). Sedimentation equilibrium studies of HMM in 0.3 M and in 20 mM NaCl indicate that both 7.5S and 9S forms are monomeric, having molecular weights of 350,000. The Mg(II) ATPase activity of HMM, without actin, decreases sharply below 0.3 M NaCl, closely paralleling the increase in S20,w. With phosphorylated HMM both the decrease in activity and the increase in S20,w occur at lower NaCl concentrations. Subfragment-1 undergoes no changes in S20,w or ATPase activity, analogous to those of the 7.5S-9S transition as judged by effects of phosphorylation and ionic strength. Electron micrographs of HMM indicate that the heads tend either to point away from the tail (extended form) or bent back towards the tail (flexed form). In 1 M NH_4OAc, where HMM in solution sediments at 7.5S, at least 90% of the molecules are in the extended form, while in 25 mM NH_4OAc (S20,w=9) the fraction of molecules in the flexed form increases to about 60%. The average length of the heads of HMM is 20 nm and that of the tail, the subfragment-2 region, is 45 nm. There is no apparent change in the shape of the head in response to phosphorylation. In 20 mM NaCl (S20,w=9) HMM is digested by papain three times faster than in 0.4 M NaCl (S20,w=7.5). ATP reduces the digestion rate in 20 mM NaCl by 90%, but has little effect in 0.4 M NaCl.

T-AM-F3 HETEROGENEITY IN SMOOTH MUSCLE SUBFRAGMENT-1. Pramod Dash and David D. Hackney, Department of Biological Sciences, Carnegie-Mellon University, Pittsburgh, PA 15213.

When assayed at high ionic strength in the presence of an ATP regenerating system, the ATPase rate of smooth muscle (chicken gizzard) myosin increases linearly up to a sharp break at the equivalence point of one ATP per myosin head group in agreement with the results of Ikebe et al., Biochem. 22, 4580 (1983). In this titration, the free ATP level is essentially zero until above the equivalence point of one ATP per myosin head group. Papain subfragment-1 (S1), however, does not follow this simple pattern. The ATPase titration is not linear at all myosin concentrations, and the break in free ATP occurs significantly below the break in the ATPase rate. This apparent heterogeneity in the titration of S1 is supported by ^{18}O-exchange data. At sub stoichiometric ATP levels, myosin hydrolyzes ATP with a very high extent of exchange, but hydrolysis by S1 is heterogeneous with a significant low exchange component. The heterogeneity in the exchange pattern of S1 becomes even more pronounced at higher ATP levels.

Supported by grant AM 25980 from the USPHS and by an Established Investigatorship from the American Heart Association to DDH.

T-AM-F4 MECHANISM OF SMOOTH MUSCLE MYOSIN PHOSPHORYLATION. Kathleen M. Trybus and Susan Lowey, Rosenstiel Center, Brandeis University, Waltham, MA 02254.

In vertebrate smooth muscles, phosphorylation of the regulatory light chain appears to be necessary for actin activation of the MgATPase activity, and for the in vitro assembly of myosin into filaments. From a correlation between the degree of phosphorylation and enzymatic activity, it was suggested that both heads of myosin need to be phosphorylated before that molecule can be activated by actin, and that phosphorylation of filamentous myosin occurs by a negatively cooperative process. Here we have attempted to determine the mechanism of phosphorylation directly by separating myosin species containing 0, 1 or 2 heads phosphorylated. The different structural properties of dephosphorylated and phosphorylated myosin in the minifilament buffer system provided the basis for this separation. Myosin minifilaments which are fully phosphorylated remain intact upon addition of MgATP, whereas dephosphorylated minifilaments are dissociated to a 15S species consisting primarily of folded dimers. Minifilaments formed from myosin with intermediate levels of phosphorylation can be separated from 15S by gel filtration. By measuring the relative amount of myosin that forms minifilament and dimer, and the degree of phosphorylation of these two species relative to the starting level of phosphorylation, it is possible to deduce the mechanism of phosphorylation. Alternatively, native gel electrophoresis can be used to separate myosin species containing different levels of phosphorylation. Taken together, these data are consistent with a model in which myosin light chain kinase phosphorylates myosin in a random manner, independent of the state of aggregation of the myosin. (Supported by an NIH fellowship to K.T. and grants from NIH, NSF and MDA to S.L.).

T-AM-F5 STRETCH-INDUCED MYOSIN LIGHT CHAIN PHOSPHORYLATION AND STRETCH-RELEASE-INDUCED TENSION DEVELOPMENT IN ARTERIAL SMOOTH MUSCLE. Kate Bárány, Ronald F. Ledvora, Sándor Csabina, and Michael Bárány. Department of Physiology and Biophysics, and Department of Biological Chemistry, College of Medicine, University of Illinois at Chicago, Chicago, IL 60612.

Helical strips from porcine carotid arteries were mounted in muscle chambers for tension measurements. Stretching to 1.7 times the resting length of arteries reversibly prevented active tension development by K^+ or norepinephrine stimulation. Myosin light chain phosphorylation was determined by two-dimensional gel electrophoresis. In the stretched noncontracting muscle phosphorylation was maximal, equal to that in nonstretched contracting muscle challenged by K^+ or norepinephrine. Stretching alone elicited light chain phosphorylation in a graded fashion reaching a plateau at 1.7 times the resting length. The same maximal level of phosphorylation was obtained in either the absence or the presence of stimulating agents. Releasing the stretch from the arteries spontaneously produced active tension. This stretch-release-induced tension approached the same magnitude as that of the control K^+-induced tension. Thus, stretching can activate arterial smooth muscle: it can induce light chain phosphorylation, and its release can induce tension development without any exogenous stimulating agent. Prolonged EGTA treatment of arteries abolished stretch-induced phosphorylation and subsequently prevented tension development upon release of the stretch. However, when EGTA was washed out and the strips were restretched and released again, the stretch-induced phosphorylation and the stretch-release-induced tension were restored. The above data may have physiological significance in the regulation of arterial blood pressure. (Supported by NIH AM 34602-10 and Chicago Heart Association).

T-AM-F6 THE EFFECTS OF AN EXOGENOUS PHOSPHATASE ON ISOMETRIC FORCE MAINTENANCE AND MYOSIN PHOSPHORYLATION OF GLYCERINATED UTERINE SMOOTH MUSCLE, Joe R. Haeberle, David R. Hathaway, and Anna A. DePaoli-Roach, Depts. Physiology, Medicine, and Biochemistry, Indiana Univ. Sch. Med., Indianapolis, IN 46223.

The hypothesis that slowly cycling "latch-bridges" form as the result of the dephosphorylation of attached crossbridges in the presence of calcium has been tested using a "skinned" uterine smooth muscle preparation. Purified catalytic subunit of a type 2A skeletal muscle protein phosphatase was added to the contracted skinned muscles to a final concentration of 0.4 uM in the presence of saturating calcium and calmodulin. Myosin phosphorylation and isometric force decreased, respectively, from 0.52 ± 0.09 mol PO_4/mol LC20 and 12712 ± 3201 N/m^2 before the addition of phosphatase to 0.15 ± 0.02 mol PO_4/mol LC20 and 3146 ± 1946 N/m^2 after the addition of the phosphatase (mean $\pm$ SD). This significant and proportional decrease in both force and myosin phosphorylation was completely reversed by the removal of exogenous phosphatase. The reduction in both isometric force and LC20 phosphorylation was also reversed by the addition of purified chicken gizzard myosin light chain kinase or thiophosphorylated chicken gizzard LC20. Thiophosphorylation of the skinned uterine muscle resulted in the incorporation of 1.0 mol PO_4/mol LC20 with an associated 2-fold increase in isometric force compared to the control muscle. Addition of the phosphatase to the muscle bath following thiophosphorylation had no effect on force maintenance or myosin phosphorylation. These results demonstrate that dephosphorylation of myosin in contracting skinned uterine smooth muscle in the presence of calcium does not result in the formation of a "latch state" where isometric force is maintained in the absence of elevated myosin phosphorylation. Moreover, isometric force was proportional to myosin phosphorylation under all conditions. This work was supported by grants from the American Heart Association, Indiana Affiliate; the NIH (HL 06308); the Juvenile Diabetes Foundation (A.D.R.) and the Herman C. Krannert Fund.

T-AM-F7 VASCULAR SMOOTH MUSCLE CALDESMON: ACTIN-BINDING PROPERTIES AND EFFECTS ON SKELETAL MUSCLE ACTO-HMM ATPase ACTIVITY. J.A.Lash, J.R.Haeberle and D.R.Hathaway, Depts. Medicine and Physiology, Ind. Univ. School Med., Indianapolis, IN.

A major calmodulin-binding protein, caldesmon, has been purified from bovine vascular smooth muscle. Approximately 20 mg of protein could be purified from 1 kg of aortas with a 30% yield. Simultaneous purification of the bovine vascular myosin light chain kinase (MLCK;10mg/kg;25%yield) indicates that vasculature contains approximately twice as much caldesmon as MLCK. Caldesmon ran as a single polypeptide (M_r=145,000) by SDS-PAGE. The protein could be chemically cross-linked (1,10-phenanthroline) to form a higher molecular weight species (M_r=290,000) suggesting that caldesmon is a dimer. Caldesmon bound to actin achieving saturation at a caldesmon:actin ratio of 1:10 in the presence or absence of tropomyosin. In the presence of tropomyosin (tropomyosin:actin,1:7), there was an approximate 10-fold increase in the affinity of caldesmon for actin. In the presence of saturating Ca^{2+} (0.1 mM), calmodulin (10 uM) decreased the affinity of caldesmon for actin 10-fold but this effect could be overcome by high concentrations of actin. Caldesmon was a potent inhibitor of skeletal muscle acto-HMM ATPase activity but only in the presence of tropomyosin. Complete suppression of ATPase activity was obtained at a caldesmon:actin molar ratio of about 1:10. There was no effect of caldesmon on the binding of skeletal HMM to actin in the presence of ADP or ATP. Our study suggests that caldesmon could serve as an actin based inhibitor of actomyosin ATPase activity in vascular smooth muscle.

T-AM-F8 SMOOTH MUSCLE CALMODULIN-BINDING PROTEINS. Philip K. Ngai and Michael P. Walsh, Department of Medical Biochemistry, University of Calgary, Calgary, Alberta, Canada T2N 4N1.

A group of smooth muscle calmodulin-binding proteins has been isolated from chicken gizzard using calmodulin-Sepharose affinity chromatography. Two major proteins in this group were identified as caldesmon and myosin light chain kinase; their tissue concentrations were determined to be 11.1 μM and 4.6 μM, respectively. Other proteins in this group, which are present at much lower tissue concentrations, included a Ca^{2+}, calmodulin-dependent caldesmon kinase, a myosin light chain kinase of M_R 104,000 (a proteolytic fragment of the native enzyme of M_R 136,000) and a number of unidentified calmodulin-binding proteins of M_R 89,000, 72,000, 37,000 and 35,000. Caldesmon lacked myosin light chain kinase and phosphatase activities and exhibited an amino acid composition quite distinct from that of myosin light chain kinase. Caldesmon did not compete with either myosin light chain kinase or cyclic nucleotide phosphodiesterase (both calmodulin-dependent enzymes) for available calmodulin. As we reported earlier (Ngai, P.K. and Walsh, M.P. (1984) J. Biol. Chem. 259, in press), caldesmon could be phosphorylated by a Ca^{2+}, calmodulin-dependent caldesmon kinase and dephosphorylated by a phosphatase. The caldesmon kinase has been purified and its activity correlated with a protein of subunit M_R 93,000. The M_R 72,000 calmodulin-binding protein is distinct from caldesmon or myosin light chain kinase and therefore appears to be a novel calmodulin-binding protein of smooth muscle. This protein inhibited myosin light chain kinase activity by a mechanism not involving simple competition for available calmodulin and may therefore play a role in regulating myosin phosphorylation. (Supported by grants from the Medical Research Council of Canada and the Alberta Heritage Foundation for Medical Research).

T-AM-F9 IMMUNOLOGICAL PROPERTIES OF MYOSIN LIGHT CHAIN KINASES (MLCK). Primal de Lanerolle, Masakatsu Nishikawa, Ruth Felson and Robert S. Adelstein, Laboratory of Molecular Cardiology, NHLBI, NIH, Bethesda, MD 20205.

We have studied the biochemical and immunological properties of MLCK. Immunoprecipitation experiments using affinity-purified antibodies to turkey gizzard MLCK demonstrated that MLCK in various avian and canine smooth muscles have M_r = 130,000 and 155,000, respectively. These antibodies neither immunoprecipitate, bind to antigenic determinants (using immunofluorescence techniques) nor inhibit MLCK activity in extracts prepared from avian and canine skeletal muscles. Experiments performed with MLCK purified from turkey gizzard (M_r = 130,000) and bovine tracheal (160,000) smooth muscles and from human platelets (M_r = 100,000) demonstrated the following: (a) one-dimensional peptide maps of S. aureus V8 protease digests showed peptides of different M_r for the gizzard and tracheal digests, while the tracheal and platelet digests contain peptides of similar M_r; (b) two-dimensional peptide maps of tryptic peptides from MLCK phosphorylated by the catalytic subunit of cyclic AMP-dependent protein kinase showed that the same sites are apparently phosphorylated on all three MLCK; (c) an Elisa assay demonstrated the binding of a third as many antibodies to tracheal MLCK as compared to the gizzard enzyme; (d) the catalytic activity of all three MLCK are inhibited at approximately the same Ab:MLCK ratio. These data demonstrate that skeletal MLCK is very different immunologically from smooth muscle and non-muscles MLCK. In addition, certain site(s) that are important for activity in the purified MLCK appear to be preserved and recognized equally well by the antibodies to turkey gizzard MLCK although there are some differences in the biochemical and immunological properties of smooth muscle MLCK.

T-AM-F10 STUDIES ON THE PHOSPHORYLATION DOMAINS OF SMOOTH MUSCLE MYOSIN LIGHT CHAIN KINASE. M. Elizabeth Payne, Marshall Elzinga*, William Anderson, Jr., and Robert S. Adelstein, Laboratory of Molecular Cardiology, NHLBI, NIH, Bethesda, MD 20205, *Brookhaven National Lab.

Turkey gizzard myosin light chain kinase can be regulated by calcium, calmodulin and by phosphorylation. Cyclic AMP-dependent protein kinase can catalyze the incorporation of up to 2 mols P/mol myosin light chain kinase, which results in a concomitant decrease in activity. The amino acid sequence of the sites phosphorylated by cAMP-dependent protein kinase is being determined. Limited digestion of ^{32}P-myosin light chain kinase with trypsin releases a labeled 23,200-dalton fragment. Following purification, the phosphopeptide is then subfragmented with Staphylococcus aureus protease. A peptide with a molecular weight of approximately 2000 daltons containing both phosphorylation sites was purified using a combination of gel filtration and reversed-phase high performance liquid chromatography. This peptide has the following amino acid composition: 3-Asp, 1-Thr, 3- or 4-Ser, 2-Glu, 2-Pro, 2-Gly, 2-Ala, 1-Val, 1-Ile, and 2-Lys.

T-AM-F11 LOW-ANGLE PLATINUM SHADOWING OF SMOOTH MUSCLE MYOSIN LIGHT CHAIN KINASE. Maryanne Vahey, M. Elizabeth Payne and Robert S. Adelstein, Laboratory of Molecular Cardiology, National Heart, Lung, and Blood Institute, NIH, Bethesda, MD 20205.

In smooth muscle and a variety of non-muscle cells, phosphorylation of the 20,000-dalton light chain of myosin by myosin light chain kinase is an obligatory step for the interaction of actin and myosin in vitro. Turkey gizzard smooth muscle myosin light chain kinase has been studied extensively with respect to its physical, hydrodynamic and kinetic properties. The data gathered from indirect hydrodynamic studies predict an asymmetric structure for the enzyme but are unable to describe morphological intricacies that direct observation should allow. In order to obtain information on the ultrastructural features of the enzyme, we initiated the present study using low-angle platinum shadowing of turkey gizzard smooth muscle myosin light chain kinase molecules dried from glycerol. Rotary and fixed-angle platinum shadowing of purified turkey gizzard myosin light chain kinase reveals that the molecule assumes at least three ultrastructural geometries. The predominant morphology is that of a 31.1 $\pm$ 4.35 nm (n = 250) contour length crescent. A linear or extended form of 47.6 $\pm$ 2.95 nm (n = 250) in length and a globular or convoluted shape of 16.0 $\pm$ 2.27 nm (n = 250) in diameter are also observed. These various presentations of myosin light chain kinase may be derived from contortions of a highly flexible linear molecule in solution. The unexpected finding that the molecule is not only asymmetric but also highly flexible poses the possibility that the interaction of this regulatory protein with its substrate, as well as with Ca^{2+}-calmodulin and cAMP-dependent protein kinase may be mediated in part by morphological changes in gizzard kinase itself.

T-AM-F12 INDEPENDENT STIMULATION OF THE ACTIN-ACTIVATED ATPases OF THE TWO HEADS OF THYMUS MYOSIN. Paul D. Wagner and Ngoc-Diep Vu, Laboratory of Biochemistry, NCI, NIH, Bethesda, MD 20205.

A nonmuscle myosin was isolated from calf thymus and the effect of phosphorylation of its 20,000 dalton light chains examined. When electrophoresed in 40 mM sodium pyrophosphate on 4% polyacrylamide gels, thymus myosin with two phosphorylated light chains migrated more quickly than unphosphorylated myosin or myosin with one phosphorylated light chain. Myosin with one phosphorylated light chain migrated only slightly faster than the unphosphorylated myosin. Thymus myosin was phosphorylated with gizzard myosin light chain kinase at low ionic strength where the myosin is filamentous and at high ionic strength where it is monomeric. Myosin with different levels of light chain phosphorylation were run on native gels, and the fraction containing two phosphorylated light chains determined. Both monomeric and filamentous thymus myosin appear to be phosphorylated randomly.

The actin-activated ATPases of thymus myosin with different levels of light chain phosphorylation were also determined. A linear relationship was obtained between the level of light chain phosphorylation and stimulation of the actin-activated ATPase. Since the two heads of thymus myosin are phosphorylated randomly, this linear relationship shows that the phosphorylation of one head of thymus myosin stimulates the actin-activated ATPase of that head independent of the phosphorylation of the second head. In contrast, both heads of gizzard myosin need to be phosphorylated before the ATPase of either head is activated by actin.

T-AM-G1 Na+ CHANNELS IN SCHWANN CELL AND AXON MEMBRANES IN RABBIT SCIATIC NERVE. S.Y. Chiu*, P. Shrager and J.M. Ritchie*, Dept. of Pharmacology, Yale Univ. School of Medicine, New Haven, CT 06510 and Dept. of Physiology, Univ. of Rochester, Rochester, NY 14642.

Schwann cells from sciatic nerves of newborn rabbits were maintained in culture for up to two weeks. Ionic conductances were analyzed by whole cell and outside-out excised patch clamp recording. Tetrodotoxin-sensitive Na^+ currents with peak values up to 2 nA were recorded from single Schwann cells. Decay kinetics of whole cell currents were highly voltage dependent in the range of -40 to 0 mV. Current-voltage curves yielded a single channel conductance of 20 pS and a reversal potential of +57 mV, close to the calculated E_{Na} of +42 mV. Exponential functions were fitted to sums of single channel sweeps and time constants of decay were very similar to those of whole cell currents. Cumulative open time histograms were well-fitted by single exponential functions. In contrast to whole cell inactivation, time constants were small (~300 μs) and independent of V_m. Schwann cell Na^+ channels are thus similar in this respect to those of several mammalian excitable cells (Aldrich et al., Nature 306: 436, 1983). We have compared Na^+ channels from Schwann cells with those from the axons they normally myelinate. Slopes of peak I-V (activation range) and h_∞ curves are similar in these cells, but activation in Schwann cells is shifted about 40 mV in the depolarizing direction from the corresponding axon curve. Rabbit Schwann cells also contain 4-aminopyridine sensitive K^+ channels with a single channel conductance of 19 pS and kinetics similar to those of neurons. We suggest that Schwann cells may serve to synthesize and insert Na^+ channels and K^+ channels in nodal and internodal axolemma, respectively. Sponsored by NIH grants NS 17965, NS08304 and NS12327 and MS Society Grant RG 1162.

T-AM-G2 SODIUM CHANNELS IN SKELETAL MUSCLE ARE PRESENT AT HIGHER DENSITY NEAR THE NEUROMUSCULAR JUNCTION. Kurt G. Beam[1], John H. Caldwell[2], and Donald T. Campbell[2]. [1]Dept. of Physiology and Biophysics, Univ. of Iowa, Iowa City, IA, [2]Depts. of Molecular and Cellular Biology, National Jewish Hospital, and Physiology, Univ. of Colo. Med. Ctr., Denver, CO.

We have used the loose patch clamp technique (Stuhmer and Almers, P.N.A.S. 79, 946-950) to measure sodium currents in 5-10 μm membrane patches at varying distances from the endplate region of skeletal muscle fibers. We used twitch fibers of the garter snake obliquus externus muscle, and enzymatically dissociated fibers from the flexor digitorum brevis muscle of the rat, since in both preparations it is possible to visualize the endplate clearly and to follow a single fiber over a considerable length. Na currents were recorded from each patch for a sequence of test pulses of increasing amplitude. In both snake and rat the currents recorded near the endplate were much larger than those recorded far away. Thus, in 5 snake fibers the ratio of peak sodium current density at sites $\leq$40 μm from the endplate, to sodium current density at sites $\geq$245 μm, was 5.5±2.4 (mean±s.d., range 1.8 to 7.7, total of 14 near sites and 16 far sites). In 4 rat fibers the ratio of peak sodium current density at sites $\leq$30 μm from the endplate, to sodium current density at sites $\geq$140 μm, was 6.0±2.1 (range 3.7 to 8.6, total of 7 near sites and 7 far sites). The increased density declined rapidly with distance from the endplate: the length constant was about 80-90 μm for the snake fibers and about 30 μm for the rat fibers. These results suggest that factors similar to those responsible for concentrating acetylcholine receptors near the endplate may also operate to concentrate sodium channels. Supported by NIH grants NS14901 (KGB) and NS16922 (JHC) and grants from MDA to KGB and DTC.

T-AM-G3 **INCREASED NA^+ CURRENT DENSITY NEAR ENDPLATES IN SNAKE SKELETAL MUSCLE.** W.M. Roberts and W. Almers. Department of Physiology and Biophysics, Univ. of Washington, Seattle, WA 98195.

We have used the loose-patch voltage clamp method (Stühmer, Roberts, and Almers in Single Channel Recording, eds. Sakmann & Neher, Plenum, 1983) to investigate the distribution of Na^+ currents (I_{Na}) near endplates on twitch fibers of the costocutaneous muscle of garter snakes. Patch areas were calculated from the apparent orifice diameter in end-on micrographs of pipettes. Electrodes (10-15 um diameter) positioned more than 60 um longitudinal distance from the endplate recorded an average peak I_{Na}=10 mA/cm². Electrodes closer than 30 um from the terminal, but not appearing to cover the highly infolded terminal membrane itself, recorded average peak I_{Na}=25 mA/cm². High current densities were also recorded on the opposite side of the fiber from the endplate. Electrodes placed over the terminal recorded larger Na^+ currents and often evoked muscle contraction. To test the possibility that differences in current density reflect different membrane areas under the pipette, we used Sylgard-coated electrodes and measured patch capacitance (C_m) by signal averaging the transient response to 10 mV steps with the electrode sealed on a muscle fiber or Sylgard. Apparent C_m's for three electrodes averaged 5.2 uf/cm², indicating a substantial contribution from membrane in the T-tubules or under the pipette rim. C_m's did not usually vary by more than 20% in different patches if the pipette did not overlap the endplate. Na^+ currents had similar voltage dependence and gating kinetics regardless of their location relative to the endplate and were blocked by 100 nM tetrodotoxin. The most striking difference between snake Na^+ channels and those studied in frog and mammalian skeketal muscle was the absence of prominent very slow components of inactivation. Supported by NIH grant AM17803.

T-AM-G4 TEMPERATURE DEPENDENCE OF SODIUM CURRENTS IN RABBIT SKELETAL MUSCLE MEMBRANE.

G.E. Kirsch, Dept. of Biol. Sci., Rutgers University, New Brunswick, NJ 08854. The effect of temperature on the kinetics of sodium (Na) channel conductance was determined in voltage-clamped rabbit skeletal muscle fibers, isolated from normal and denervated muscles. The Hodgkin-Huxley model was used to extract kinetic parameters; the time course of the conductance change after step depolarization (from -100 to -20 mV) followed m^3h kinetics. Arrhenius plots of Na channel activation (log (tau m) vs. 1/temperature) were linear (activation energy, E_a = 72.5 kJ/mole) in the temperature range 0 to 22 deg. C (temperature coefficient, Q_{10} = 2.9). In contrast, the temperature dependence of inactivation (tau h) was non-linear such that Q_{10} values of 3.0 and 5.7 (corresponding to E_a = 77.7 and 110.0 kJ/mole), respectively, were required to fit the data near the high and low temperatures within this range. No breakpoints or hysteresis were observed. Similar results were obtained for the tetrodotoxin-sensitive Na conductances in normal and denervated fibers. The effect of cooling on inactivation time course is similar in magnitude to that observed for potassium channel activation in rat muscle (Beam and Donaldson, 1983) but much less than that of Na inactivation in rabbit node of Ranvier (Chiu, et al., 1979). These results support the notion that channel-lipid interactions in mammalian muscle differ from those in myelinated nerve and clearly indicate that when comparing the inactivation time course of mammalian muscle Na channels, the use of a single Q_{10} for scaling kinetic parameters over a broad temperature range is inappropriate. Supported by MDA and NIH grant NS17799.

T-AM-G5 Na-CHANNEL BLOCK BY u-CONOTOXIN GIIIA: A PEPTIDE TOXIN SPECIFIC FOR SKELETAL MUSCLE.

Edward G. Moczydlowski, Dept. of Physiology and Biophysics, Univ. of Cincinnati College of Medicine, Cincinnati, OH 45267.

The electrophysiological literature contains numerous reports of toxins that have selective action on Na-current with respect to species, tissue and developmental changes. One example is a group of peptide toxins from the marine snail Conus geographus that are reported to abolish muscle action potentials while having no effect on nerve firing or endplate potentials. The purified toxin GIIIA is a peptide of 22 amino acids containing 8 lys + arg, 6 cys and 3 hydroxyproline residues (S. Sato et al 1983, FEBS Lett. 155, 277; D.L. Stone and W.R. Gray 1982, Arch. Biochem. Biophys. 216, 765; L.J. Cruz et al, submitted to J. Biol. Chem.) The action of this toxin was examined on single batrachotoxin-activated Na-channels incorporated into planar lipid bilayers from membrane preparations of rat muscle or rat brain. u-Conotoxin GIIIA induced the appearance of long-lived blocked states in muscle Na-channel records. Block was only observed when GIIIA was present on the extracellular channel surface and the kinetics could be described as a reversible binding equilibrium. At 0 mV and 22°C the mean blocked time was 140 seconds and the derived equilibrium dissociation constant was 100 nM. The voltage dependence of blocking rates was similar to that previously observed for tetrodotoxin and saxitoxin in planar bilayer experiments. In contrast to the results for muscle channels, GIIIA had no effect on Na-channels from rat brain . In conclusion, it appears that u-conotoxin is able to discern structural differences between nerve and muscle Na-channels.

T-AM-G6 SLOW CURRENTS THROUGH SKELETAL MUSCLE Na^+ CHANNELS ARE NOT "WINDOW CURRENTS". **Joseph Patlak and Mauricio Ortiz. Dept. of Physiology, University of Vermont, Burlington, VT. 05405.**

We recorded currents at moderate depolarization from Na^+ channels of tissue cultured rat skeletal muscle. Cells were bathed in a Hi-K^+ solution that reduced the cells' resting potential to low values. Patch recordings were made in the "cell attached" configuration at 11° C. The electrode contained physiological saline. Currents were filtered at 500 Hz and sampled once every ms. Membrane patches were hyperpolarized to -120 or -140 mV to remove all inactivation. 150 ms pulses were given at 1 Hz to potentials from -60 to 0 mV. Channels opened quickly at the start of the pulse, then closed after several ms. The mean current also decayed within several ms, indicating that channel reopenings were rare. Late currents through Na^+ channels were similar to those which we have observed in cardiac muscle [Patlak and Ortiz, Slow Currents Through Single Sodium Channels of the Adult Rat Heart, J. Gen. Physiol, submitted]. In one patch with 4-5 channels 10% of all pulses had currents that continued after fast inactivation was complete. These currents consisted of repeated openings and closings (bursts) of a single channel. Mean duration of the bursts was 32 ms and several lasted more than 100 ms. At -30 mV pulse potential both the mean open and closed times during the burst were longer than those that compose the fast Na^+ currents. In other patches the bursts were similar, but occured less frequently. These currents are fundamentally different from "window currents", in which the channel returns from inactivation, functions briefly as it did at the start of the pulse, and then re-inactivates. The highly grouped openings that we observe must be caused by a Na^+ channel that is functioning in a different set of states as at the start of the pulse. **Supported by NIH grant HL-28192.**

T-AM-G7 SINGLE CHANNEL AND PSEUDOMACROSCOPIC ANALYSIS OF QX-314 BLOCKING ACTION ON Na CHANNELS IN NEUROBLASTOMA CELLS. William A. McCarthy, Jr. and Jay Z. Yeh, Dept. of Pharmacology, Northwestern University Medical School, Chicago, IL 60611.

The effects of QX-314 on single Na channels were studied using the gigohm seal patch clamp technique on excised inside-out patches of N1E-115 neuroblastoma cells. Depending on the number of channels in the patch, both pseudomacroscopic (PM) currents (> 15) and single channel (SC) currents (1-5) were studied. When QX-314 (70-100 μM) was applied to the bath, it produced a resting and frequency-dependent block of the PM Na current. No difference was observed in the kinetics of decay of the current in these two types of block, and these kinetics were slightly prolonged relative to the control at larger depolarizations. It also caused a small but consistent delay of the time to peak of the current. SC data also showed a decrease in the frequency of channel opening with QX-314 present, but no significant change in SC conductance. SC first latency data showed a population of late-opening channels (first latency > 50 ms) in the presence of drug. In contrast to 9-aminoacridine, no flickering behavior was observed in the presence of QX-314, even though both agents have similar effects on the macroscopic Na current. QX-314 caused the appearance of an additional exponential component in the cumulative open time distribution, with a much larger time constant than that of the control. This was seen as occasionally occuring greatly prolonged SC events. Given that the SC conductance was not affected by QX-314, we interpret the resting and frequency-dependent block to be due to the decrease in the frequency of channel opening caused by the drug. The delay in the time to peak, and the late-opening channels, suggest that QX-314 might stabilize a closed state of the channel, slowing its opening rate. Supported by NIH grant GM-31458.

T-AM-G8 DIMERS OF BATRACHOTOXIN-MODIFIED SODIUM CHANNELS
K. Iwasa, G. Ehrenstein, and N. Moran, Lab of Biophys. NINCDS, NIH bldg. 36, room 2A-29, Bethesda, Maryland 20205.

It has been commonly assumed that ionic channels of the same kind on a membrane patch are identical and independent, and that the probability distribution of the number of open channels is binomial. Although these assumptions appear reasonable, no systematic examination of ther validity has been reported so far. We have tested these assumptions in the simplest case, patches which contain two batrachotoxin (BTX)-modifed sodium channels. First, current records from voltage clamped membrane patches which contained two batrachotoxin-modified sodium channels were analyzed to determine the relative probabilities that zero, one, or two channels were open. The experimental probabilities do not fit the binomial distribution, indicating that the two channels are non-identical or non-independent. Second, from the same current records, we also determined the rate for the transition from two open channels to one open channel and for the transition from one open channel to zero open channels. A detailed comparison of the open probabilities and the closing rates of two-channel and one-channel patches leads to the conclusion that the two channels are non-independent. More specifically, the opening rates of a chennel are higher when the other channel in the same patch is closed than it is open.

T-AM-G9 VOLTAGE-DEPENDENT GATING OF SINGLE BATRACHOTOXIN-ACTIVATED SODIUM CHANNELS IN PLANAR BILAYERS. R. J. French*, M. B. Blaustein**, W. O. Romine**, K. Tam*, J. F. Worley, III** and B. K. Krueger**. Departments of Biophysics* and Physiology**, University of Maryland School of Medicine, Baltimore, Maryland 21201.

Single batrachotoxin-activated sodium channels incorporated into lipid bilayer membranes fluctuate between the open and closed states over a wide range of voltages. As the membrane is hyperpolarized from -70 mV to -100 mV the channels change from being mostly open to mostly closed. Apparent gating charge, determined from the steady state activation curve (a plot of fractional open time vs. voltage), is 4-6 e/channel. Open time distributions are well-fit by a single exponential, suggesting a single open state. From the voltage dependence of the open times, an effective gating charge of 1-1.5 e/channel may be associated with the unidirectional closing transition. Closed time distributions suggest more than one step in the opening sequence. Studies of the gating process are complicated by occasional non-stationarity of the current fluctuations. At a constant voltage, a channel may abruptly switch from being mostly open to being mostly closed, and then continue in a new pseudosteady state for many seconds. Sometimes, the fluctuations appear to remain stationary at a constant voltage. Gating activity can be modulated by calcium ions. Addition of calcium to the external solution causes a shift of the activation curve toward more depolarized potentials (i.e. the channel remains closed more of the time). This shift may be reversed by addition of calcium to the internal solution. These effects may be due to modification or screening of the surface charge on either the channel protein or on the surface of the lipid membrane. Supported by NIH grants NS16285 and NS20106, U.S. Army Medical Research and Development Command, and by a Graduate Fellowship and a Short Term Research Program Fellowship from the University of Maryland.

T-AM-G10 CHARACTERIZATION OF TWO TYPES OF TETRODOTOXIN RECEPTORS IN ISOLATED FROG MUSCLE MEMBRANES. Enrique Jaimovich, José Luis Liberona and Cecilia Hidalgo[a], Depto. Fisiol. y Biofis., Fac. de Med., U. de Chile, and [a]Muscle Dept., Boston Biomed. Res. Inst. and Dept. Neurol., Harvard Med. Sch., Boston, MA 02114.

Two different methods were used to isolate membrane fractions from frog skeletal muscle. In one method, a light membrane fraction of transverse tubule origin was obtained which contained a homogeneous population of receptors for tritiated derivatives of tetrodotoxin (Kd = 0.3 nM). The second procedure, using a high ionic strength KBr extraction, yielded a fraction of purified membranes with two families of tetrodotoxin receptors (K_1d = 0.3 nM, K_2d = 5 nM). Modification of these latter membranes using the amino group reagent trinitrobenzenesulfonate produced a reduction of the maximal binding capacity for tetrodotoxin. This effect depended on the concentration of trinitrobenzenesulfonate used (10^{-4} to 10^{-2} M) and could be prevented by incubation with unlabeled tetrodotoxin. Trinitrobenzenesulfonate treatment did not affect the dissociation constant of the high affinity receptors, and selectively inhibited the low affinity tetrodotoxin binding at concentrations at which the high affinity receptors remained unchanged. Treatment with saponin showed that most vesicles are sealed, the proportion of non-accessible high affinity receptors being higher than that of the low affinity receptors.

Supported by U. de Chile DIB grant B912 and by NIH grant HL23007.

T-AM-G11 PURIFICATION AND RECONSTITUTION OF THE SINGLE,LARGE TETRODOTOXIN-BINDING POLYPEPTIDE FROM EEL ELECTROPLAX USING CHAPS DETERGENT BUFFERS. D. S. Duch & S. R. Levinson, Dept. of Physiology, U. of Colorado Medical School, Denver, Co. 80262. The tetrodotoxin-binding component (TTXR) from the eel electroplax has been solubilized with 3-[(3-cholamidopropyl)dimethylammonio]-1-propane-sulfonate (CHAPS) and purified in buffers containing CHAPS and selected lipids. In CHAPS-asolectin buffer, TTXR has been purified in high yield (35%) and specific activity (peak fractions greater than 2900 pmol of (3H)TTX bound per mg of protein). These fractions demonstrated only a single, large polypeptide on SDS-PAGE. Purification of TTXR in CHAPS-phosphatidylcholine buffer also resulted in a single, large polypeptide on SDS-PAGE, but yields and specific activities were much lower (1400 specific activity). TTXR from the CHAPS-PC purification containing the single polypeptide were reconstituted into PC(.6):PS(.2):PE(.2) vesicles by dialysis. Veratridine stimulated Na-22 flux into these vesicles was demonstrated. These fluxes were blocked by external TTX alone. These experiments provide further evidence that the sodium channel from eel electroplax consists of a single, large, compositionally complex polypeptide.

T-AM-G12 **THE IN VITRO BIOSYNTHESIS OF THE TETRODOTOXIN-BINDING COMPONENT CORE PROTEIN FROM EEL ELECTROPLAX.** **W.B. Thornhill & S.R. Levinson, Dept. Physiology, U. Colorado Medical School, Denver, CO 80262.** **RNA derived from the electroplax of Electrophorus electricus was used to direct in vitro protein synthesis in a rabbit reticulocyte lysate system. The major ^{35}S-methionine labeled proteins that were synthesized ranged in size from 12 to 200 kilodaltons when analyzed by SDS-PAGE. Rabbit antisera directed against the electroplax tetrodotoxin-binding component (TTXR, M_r approx.260,000) specifically immunoprecipitated a 230,000 dalton protein from the translation mixture. This unprocessed core protein did not a exhibit diffuse banding pattern nor an anomalously high relative free mobility when subjected to SDS-PAGE and Ferguson analysis. This is in contrast to the native TTXR which does show a diffuse banding pattern, possibly due to its heavy glycosylation, and a high relative free mobility resulting from its anomalously high binding of SDS. Thus post-translational processing of the core protein to the native form is required for its diffuse banding pattern and high binding of SDS. We infer that glycosylation of the core protein is indeed responsible for the former attribute, while fatty acid acylation is responsible for the latter. Supported by NIH NS-15879, the Muscular Dystrophy Association, and NIH RCDA NS-00529 to SRL.**